

## NRC Publications Archive Archives des publications du CNRC

### **A state-of-the-art review on ice modeling methodologies employed in refrigerated ice tanks**

Wang, J.; Lau, M.

For the publisher's version, please access the DOI link below./ Pour consulter la version de l'éditeur, utilisez le lien DOI ci-dessous.

#### **Publisher's version / Version de l'éditeur:**

<https://doi.org/10.4224/8895364>

*Laboratory Memorandum (National Research Council Canada. Institute for Ocean Technology); no. LM-2007-05, 2007*

#### **NRC Publications Archive Record / Notice des Archives des publications du CNRC :**

<https://nrc-publications.canada.ca/eng/view/object/?id=1dd4a44e-dbb8-4716-a4f2-4301610e70c4>

<https://publications-cnrc.canada.ca/fra/voir/objet/?id=1dd4a44e-dbb8-4716-a4f2-4301610e70c4>

Access and use of this website and the material on it are subject to the Terms and Conditions set forth at

<https://nrc-publications.canada.ca/eng/copyright>

READ THESE TERMS AND CONDITIONS CAREFULLY BEFORE USING THIS WEBSITE.

L'accès à ce site Web et l'utilisation de son contenu sont assujettis aux conditions présentées dans le site

<https://publications-cnrc.canada.ca/fra/droits>

LISEZ CES CONDITIONS ATTENTIVEMENT AVANT D'UTILISER CE SITE WEB.

**Questions?** Contact the NRC Publications Archive team at

PublicationsArchive-ArchivesPublications@nrc-cnrc.gc.ca. If you wish to email the authors directly, please see the first page of the publication for their contact information.

**Vous avez des questions?** Nous pouvons vous aider. Pour communiquer directement avec un auteur, consultez la première page de la revue dans laquelle son article a été publié afin de trouver ses coordonnées. Si vous n'arrivez pas à les repérer, communiquez avec nous à PublicationsArchive-ArchivesPublications@nrc-cnrc.gc.ca.

LM-  
2007-  
05

Archive copy



National Research  
Council Canada

Conseil national  
de recherches Canada

Institute for  
Ocean Technology

Institut des  
technologies océaniques

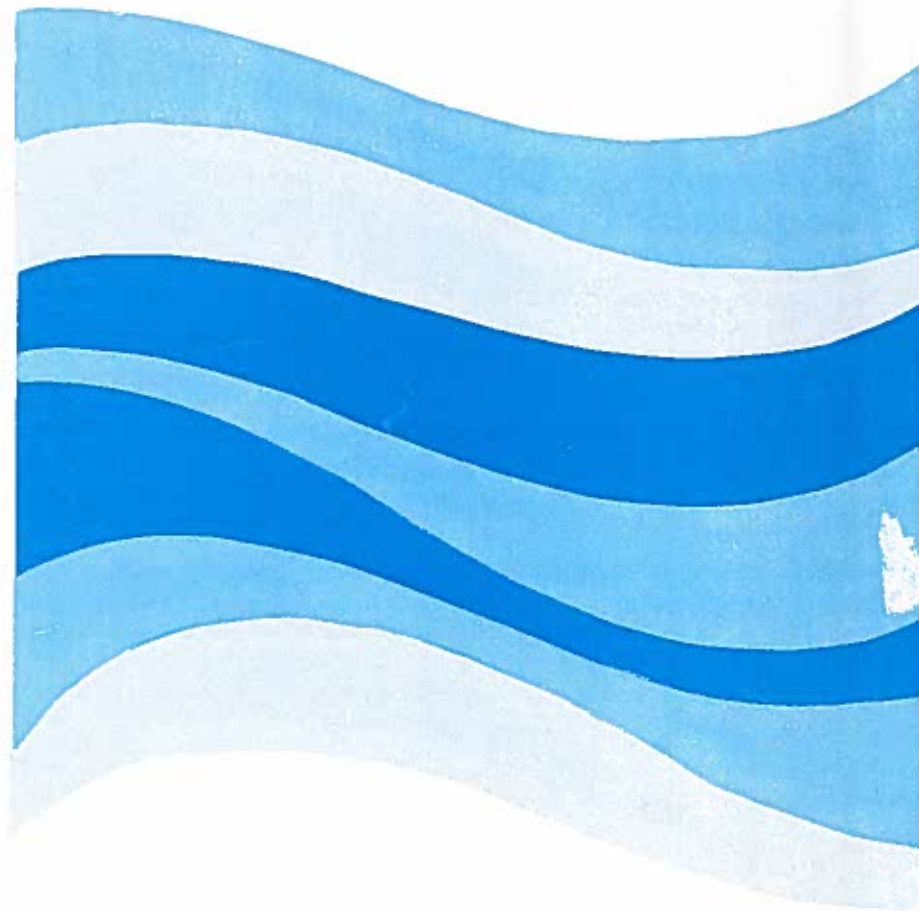
LM-2007-05

## Laboratory Memorandum

### **A STATE-OF-THE-ART REVIEW ON ICE MODELING METHODOLOGIES EMPLOYED IN REFRIGERATED ICE TANKS**

Jungyong Wang and Michael Lau

May 2007



## DOCUMENTATION PAGE

<b>REPORT NUMBER</b> LM-2007-05	<b>NRC REPORT NUMBER</b>	<b>DATE</b> May 24, 2007	
<b>REPORT SECURITY CLASSIFICATION</b> Unprotected		<b>DISTRIBUTION</b> Unlimited	
<b>TITLE</b> A state-of-the-art review on ice modeling methodologies employed in refrigerated ice tanks			
<b>AUTHOR(S)</b> Jungyong Wang and Michael Lau			
<b>CORPORATE AUTHOR(S)/PERFORMING AGENCY(S)</b> Institute for Ocean Technology			
<b>PUBLICATION</b>			
<b>SPONSORING AGENCY(S)</b> Institute for Ocean Technology & Maritime Ocean Engineering Research Institute			
<b>IOT PROJECT NUMBER</b> PJ2217		<b>NRC FILE NUMBER</b>	
<b>KEY WORDS</b> Ice Tank, Model Ice, Model Test, IOT Facility		<b>PAGES</b> 44	<b>FIGS.</b> 12
			<b>TABLES</b> 2
<b>SUMMARY</b> Recent exploration of natural resources and their transportation in the arctic or sub-arctic regions and the increase of traffic through the Northern Sea Route (NSR) have stimulated new structural concepts and ship designs. To evaluate the design and performance of these structures and ships, model tests in an ice tank are the preferred evaluation tool. The Maritime Ocean Engineering Research Institute (MOERI) is building the first ice tank in Korea to meet the increasing research and development challenges and opportunities arisen from the recent demands. This study mainly reviews the state-of-the-art ice modeling techniques and methodologies used in existing refrigerated model basins to assist their adaptation to the new ice tank. The physical and mechanical properties of different types of model ice and their scalability are critically assessed. Comparisons of mechanical properties from sea ice and model ice are presented and discussed. This report also briefly discusses scaling issues for ice model tests, test methodologies for ship performances in ice, and the ice testing facilities at IOT.			
<b>ADDRESS</b> National Research Council Institute for Ocean Technology Arctic Avenue, P. O. Box 12093 St. John's, NL A1B 3T5 Tel.: (709) 772-5185, Fax: (709) 772-2462			



National Research Council  
Canada

Conseil national de recherches  
Canada

Institute for Ocean  
Technology

Institut des technologies  
océaniques

**A STATE-OF-THE-ART REVIEW ON ICE MODELING  
METHODOLOGIES EMPLOYED IN REFRIGERATED ICE TANKS**

**LM-2007-05**

**Jungyong Wang<sup>1</sup> and Michael Lau<sup>2</sup>**

*<sup>1</sup>Faculty of Engineering and Applied Science, Memorial University of Newfoundland*

*<sup>2</sup>Institute for Ocean Technology, National Research Council of Canada*

May 24, 2007

## **ABSTRACT**

Recent exploration of natural resources and their transportation in the arctic or sub-arctic regions and the increase of traffic through the Northern Sea Route (NSR) have stimulated new structural concepts and ship designs. To evaluate the design and performance of these structures and ships, model tests in an ice tank are the preferred evaluation tool. The Maritime Ocean Engineering Research Institute (MOERI) is building the first ice tank in Korea to meet the increasing research and development challenges and opportunities arisen from the recent demands. This study mainly reviews the state-of-the-art ice modeling techniques and methodologies used in existing refrigerated model basins to assist their adaptation to the new ice tank. The physical and mechanical properties of different types of model ice and their scalability are critically assessed. Comparisons of mechanical properties from sea ice and model ice are presented and discussed. This report also briefly discusses scaling issues for ice model tests, test methodologies for ship performances in ice, and the ice testing facilities at IOT.

## TABLE OF CONTENTS

ABSTRACT.....	ii
TABLE OF CONTENTS.....	iv
LIST OF TABLES.....	v
LIST OF FIGURES.....	v
NOMENCLATURE.....	v
1. INTRODUCTION.....	1
2. HISTORIC REVIEW OF MODEL ICE.....	2
2.1. Columnar Model Ice.....	2
2.1.1. Russian experience.....	2
2.1.2. German experience.....	3
2.1.3. Canadian experience.....	3
2.1.4. American experience.....	5
2.1.5. Japanese experience.....	5
2.2. Granular Model ice.....	5
2.2.1. Finnish experience.....	5
3. MECHANICAL PROPERTIES OF MODEL ICE.....	7
3.1. Flexural Strength.....	7
3.2. Compressive Strength.....	9
3.3. Elastic Modulus.....	11
3.4. Fracture Toughness.....	12
3.5. Density.....	13
3.6. Summary of Mechanical Property of Model Ice.....	14
4. SCALING.....	16
5. TEST METHODOLOGY AND DATA ANALYSIS FOR SHIP IN ICE PERFORMANCE EVALUATIONS.....	18
5.1. Ship Resistance in Ice.....	18
5.1.1. ITTC standard method.....	21
5.1.2. IOT standard method.....	21
5.2. Propulsion in Ice.....	23
5.2.1. IOT method.....	23
5.3. Maneuvering in Ice.....	24
5.3.1. Free running model tests.....	24
5.3.2. Captive model tests.....	25
6. FACILITIES AT IOT.....	32
6.1. Ice Tank.....	32
6.2. Refrigeration System.....	33
6.3. Towing Carriage (Main Carriage).....	34
6.4. Service Carriage (Second Carriage).....	35
6.5. Air Bubble System to Correct Density.....	36
7. SUMMARY.....	38
8. REFERENCE.....	39

## LIST OF TABLES

Table 1: Refrigerated model basins and their model ice .....	6
Table 2: Summary of scaling laws according to Froude and Cauchy scaling (Timco, 1984).....	17

## LIST OF FIGURES

Figure 1: Typical flexural strength range of model ice (*: best estimated).....	8
Figure 2: Compressive strength against strain rate.....	10
Figure 3: Compressive strength against flexural strength .....	10
Figure 4: Elastic modulus vs. flexural strength (*: best estimated).....	12
Figure 5: Critical stress intensity factor vs. flexural strength.....	13
Figure 6: Typical density range of model and sea ice .....	14
Figure 7: Standard PMM tests (modified from Marineering Limited, 1997).....	28
Figure 8: Schematic diagram of the ice tank (after IOT standard test method, 2000).....	32
Figure 9: Temperature survey during the preparation of ice sheet.....	34
Figure 10: Front view of main carriage (15m long, 14.2 m wide, and 3.96 m high; after IOT standard test method, 2000).....	35
Figure 11: Front view of service carriage (after IOT standard test method, 2000) ...	36
Figure 12: Air bubble system (after Spencer and Timco 1990) .....	37

## NOMENCLATURE

### Mechanical Properties of Ice

$E$  : Elastic Modulus [MPa]

$K_{Ic}$  : Critical Stress Intensity Factor [kPa·m<sup>1/2</sup>]

$\sigma_c$  : Compressive Strength [kPa]

$\sigma_f$  : Flexural Strength [kPa]

$\lambda$  : Scale Ratio [-]

### Model Ice

- EG/AD/S model ice: Ethylene Glycol, Aliphatic Detergent, and Sugar doped model ice developed by NRC (Timco, 1986)

- CD- EG/AD/S model ice: Correct Density-EG/AD/S model ice developed by NRC (Spencer and Timco, 1990)

- FG model ice: **Fine Granular model ice** (saline solution) developed by WARC (Enkvist and Makinen, 1984)
- FG-urea model ice: **Fine Granular model ice with urea solution** developed by NKK (Narita et al, 1988)
- FGX model ice: **2nd generation FG model ice** developed by MARC (Nortala-Hoikkanen, 1990)
- GE model ice: **Granular Ethanol model ice** developed by AORC (Jalonen and Ilves, 1990)
- PG model ice: **Propylene Glycol model ice** developed by NMRI (Personal communication)

**Industry, University and Research Institute**

**AARC: Aker Arctic Technology Inc.**

**AARI: Arctic and Antarctic Research Institute**

**AORC: Arctic Offshore Research Centre**

**CHC: Canadian Hydraulics Centre in NRC**

**CRREL: Cold Regions Research and Engineering Laboratory**

**HSVA: Hamburg ship model basin**

**HUT: Helsinki University of Technology**

**IHI: Ishikawajima-Harima Heavy Industries**

**IIHR: Iowa Institute of Hydraulic Research**

**IMD: Institute for Marine Dynamics**

**IOT: Institute for Ocean Technology in NRC, formerly IMD**

**ITTC: International Towing Tank Conference**

**KSRI: Krylov Shipbuilding Research Institute**

**MARC: Kvaerner-Masa Yards Arctic Research Centre, formerly WARC**

**MHI: Nagasaki Research & Development Center**

**MOERI: Maritime & Ocean Engineering Research Institute**

**NKK: Nippon KoKan Corporation**

**NMRI: National Maritime Research Institute, formerly SRI**

**NRC: National Research Council of Canada**

**SRI: National Maritime Research Institute**

**WARC: Wartsila Arctic Research Centre, name changed to MARC in 1989**

**WIMB : Wartsila Ice Model Basin**

## 1. INTRODUCTION

Recent exploration of natural resources and their transportation in the arctic or sub-arctic regions and the increase of traffic through the Northern Sea Route (NSR) have stimulated new structural concepts and ship designs. To evaluate the design and performance of these structures and ships, model tests in an ice tank are the preferred evaluation tool. The Maritime Ocean Engineering Research Institute (MOERI) is building the first ice tank in Korea to meet the increasing research and development challenges and opportunities arisen from the recent demands.

A study to review the state-of-the-art modeling techniques and methodologies used in existing refrigerated model basins, including model ice production and ice modeling techniques, was conducted to assist their adaptation to the new ice tank. In Section 2, a historical review of model ice is presented. From the first ice tank in the 1950s, major refrigerated model ices are introduced and their characteristics are critically assessed. The mechanical properties of several different model ices including flexural strength, compressive strength, elastic modulus, fracture toughness, and density are compared and discussed in Section 3. Scaling for the model tests are briefly introduced in Section 4. In Section 5, the methodologies for model tests including resistance, propulsion, and maneuvering tests are introduced. For ship resistance tests, current methodologies recommended by the ITTC and IOT standards are presented and discussed. For propulsion and maneuvering model tests, IOT standard method is introduced. In Section 6, IOT facilities including its ice tank, main and service carriages, refrigeration system, and underwater bubble system are described.

## 2. HISTORIC REVIEW OF MODEL ICE

Reviews of model ice were published by several investigators (Jones, 1986; Timco, 1992; Zufelt and Ettema, 1996). Two types of model ice are currently in use by ice tanks in the world, which are either columnar or granular in structure. For columnar model ice, the different solutions being employed are saline, urea, and EG/AD/S. For granular model ice, saline and urea solution are used. In this section, model ice employed by different ice tanks is introduced and its characteristics are briefly summarized.

### 2.1. Columnar Model Ice

#### 2.1.1. Russian experience

In 1955, the Arctic and Antarctic Research Institute (AARI) in Russia built the first model ice basin in the world, where modeling of ice/ship interaction was performed that laid the foundation of the theory of ice resistance to ship motion and the methods for assessment and calculation of ship performance in ice (Shvaishtein, 1959). The first model ice used at AARI was made by a 3 % sodium chloride solution. This ice had salinities in the range of 10-20 ppt, higher than natural sea ice. The model ice was grown in a process similar to that which occurs in nature, using wet seeding to obtain the correct microstructure of sea ice. The chilled water (-0.1 to -0.2 °C) was sprayed into the cooled air (-10 to -14 °C) to produce a fine mist of ice crystals. These fine particles settle down on the water surface to initiate the ice growth process similar to that occurs on calm water and cold air temperature during a foggy night. These crystals grow downward to obtain the typical columnar structure of sea ice. The procedure of wet seeding has been adopted in various ice tanks to produce columnar model ice.

The mechanical properties of sea ice are a function of brine volume (Timco and O'Brien, 1994; and Timco and Frederking, 1990), which in turn is a function of ice salinity and temperature (Weeks and Assur, 1967). Furthermore, the mechanical properties of sea ice are also influenced by its grain size and crystallographic orientation (Wang, 1979a). Therefore, when these factors are properly controlled, the strength of saline model ice can be scaled down from the full-scale values (Shvaishtein, 1971). For example, an increase of temperature and salinity of ice leads to the increase of brine volume that in turn decreases the strength of model ice.

The major deficiency of saline ice as a modeling ice material is its difficulty in satisfying both the Froude and Cauchy laws simultaneously if the scale factor is large ( $\lambda > 30$ ) as shown by Schwarz (1977). Experience with the saline ice has indicated that choosing a model scale beyond 30 would lead to improper Cauchy scaling with the  $E/\sigma_f < 2000$ . This restricted the model testing at a small-scale factor ( $\lambda = 15$  to 20) (Timco, 1979).

Improved saline model ice is addressed in next section. It was reported that AARI used the saline model ice in 1990 (Jalonen and Ilves, 1990), but the salinity AARI used was not reported. In 1986, KSRI built an ice tank and used NaCl solution (12.2 ppt). At present, KSRI produces both columnar and granular model ice (Wilkman et al., 1997).

### 2.1.2. German experience

HSVA in Germany built its ice tank in 1971 and used saline water as ice growth solution. In practice, Froude law was adhered to without consideration of the proper modeling of the ice's elasticity and the ratio of its  $E/\sigma_f$  was too low (200-500) in comparing to that of sea ice (2000-5000). Consequently, the results from model tests of ship resistance in ice were too high because of residual plasticity. Schwarz (1975) suggested two methodologies to increase this ratio. The first method used a low saline solution (up to 0.67% saline concentration), which can provide better elastic properties at high air temperature (about 0°C) and the second method used a "tempering process", in which the ice was warmed up leading to reduction of its strength and increase of its  $E/\sigma$  ratio.

Most doped model ices had a residual plasticity and high density (range of sea ice density is from 0.84  $\text{Mgm}^{-3}$  to 0.94  $\text{Mgm}^{-3}$ , and range of model ice density is from 0.93  $\text{Mgm}^{-3}$  to 0.98  $\text{Mgm}^{-3}$ ). In 1993, Evers and Jochmann (1993) reported the structure and density of doped model ice grown from saline, urea and EG/AD/S solutions can be improved by using compressed air bubbles and ice scraper during the ice growth process. The air bubbles are trapped in the upper layer in order to decrease the hardness. As the ice scraper scraps the ice crystals on the bottom of the ice sheet, the fine-grained ice crystals can be produced instead of columnar structure in order to increase the hardness in the lower layer. By using air bubbles and ice scraper, the structure and grain size of the model ice could be controlled and the ice properties could be improved.

The saline model ice is of interest from a historical point of view. Its use has since been abandoned by most modeling basins in favor of urea or EG/AD/S model ice, which exhibit better scalability of its elasticity to flexural strength ratio and are less corrosive. HSVA in Germany, however, currently uses air bubbles and ice scraper with a 0.7 % sodium chloride solution to overcome the demerits of original saline model ice.

### 2.1.3. Canadian experience

In Canada, the two ice modeling basins of the National Research Council of Canada (NRC) located at the Canadian Hydraulics Centre (CHC) and the Institute for Ocean Technology (IOT, formerly IMD) were built in 1981 and 1985, respectively (Pratte and Timco, 1981; Jones 1986). The building of these two facilities led to an important research program at the NRC to search for a substitute for sodium chloride to be used in refrigeration basins (Timco, 1979).

Timco (1979) investigated the properties of ice grown from 40 dopants in an effort to alter and improve its properties. The effort resulted in the selection of carbamide (urea) at 1.3% concentration. Urea ice is nontoxic and possessed better strength and rigidity characteristics than saline ice. It has a  $E/\sigma_f$  ratio of greater than 2400 when the flexural strength is less than 20 kPa.

Timco (1980 and 1983) and Hirayama (1983) reported the results of extensive tests on the physical and mechanical properties of saline and urea-doped ice. Although the crystal structure of the urea ice is similar to that of the saline ice, the mechanical properties are substantially different. The urea ice has a greater strain modulus than that of the saline ice at a comparable flexural strength. Static steel-ice friction coefficient of both urea and saline ice is about 0.35, and it is within the range found for sea ice (0.15-0.5) at the same condition. The density of urea ice is about  $0.95 \text{ Mgm}^{-3}$  that is higher than that of the saline ice ( $0.89 \text{ Mgm}^{-3}$ ). When the scale factor is over 30, compressive strength for both types of model ice is about 2 to 3 times lower than the required values. Since the  $E/\sigma_f$  ratio plays a major role in the brittle behavior of ice, the urea model ice could be superior to the saline model ice; however, its modeling of compressive strength and density needs improvement.

In 1986, Timco (1986) introduced a new type of model ice that was grown from an aqueous solution of three different dopants - ethylene glycol (EG), aliphatic detergent (AD), and sugar (S). Reported features of EG/AD/S ice are single-layered, fine-grained, and columnar. It is noted that the EG/AD/S from IOT cannot produce a strictly single layer ice and it is possibly because of the different facilities. Timco compared the mechanical properties of EG/AD/S ice to those of the urea model ice and saline ice (Timco, 1986). The scalability of EG/AD/S ice was superior to that of the urea model ice in all aspects, including improved scaling of flexural strength, compressive strength (uniaxial and confined), failure envelope for compression, strain modulus, and fracture toughness. Timco showed brittle behavior of EG/AD/S ice after failure and a good agreement of failure envelope for compression between sea ice and EG/AD/S model ice. For the  $E/\sigma_f$  ratio, EG/AD/S model ice gives a value between 1500 to 2500 for the whole range of flexural strengths (20-100 kPa).

Although, EG/AD/S model ice shows better scalability in comparing to the urea model ice, the discrepancy between EG/AD/S and sea ice exists. For example,  $E/\sigma_f$  ratio of sea ice varies from 2000 to 8000 depending on the region and season, but EG/AD/S ice gives a ratio of about 2500. Density and fracture toughness of EG/AD/S ice is also higher than sea ice. Detailed comparison with other model ices and sea ice will be presented later in the Section 3.

In 1990, Spencer and Timco (1990) introduced an improvement to the EG/AD/S ice, called Correct Density-EG/AD/S ice. The density of this model ice was reduced to that of sea ice by trapping air bubbles in it. In addition to a better modeling of ice density, CD-EG/AD/S model ice had several advantages in comparing to EG/AD/S model ice, i.e., the improved visibility, the higher  $E/\sigma_f$  ratio, and the lower fracture toughness.

In 1994, Spencer and Hill (1994) introduced Hi-E (high elastic modulus) EG/AD/S model ice as an improved EG/AD/S model ice. Although EG/AD/S model ice produced a single layer columnar structure, the bottom of the ice sheet was relatively weak and more

elastic.<sup>1</sup> In order to strengthen the bottom layer of the model ice to increase its elastic modulus and to maintain homogeneity over its depth, “washer” unit were used to flush out the high concentration of glycol at the ice-water interface (Spencer and Hill, 1994).

At present, IOT employs both EG/AD/S and CD-EG/AD/S model ice but the latter is more often used.

#### **2.1.4. American experience**

In the United States, the U.S. Army Cold Regions Research and Engineering Laboratory (CRREL) built its ice tank in 1979, and the Iowa Institute of Hydraulic Research (IIHR) built its ice tank in 1981. Both tanks employed urea model ice (Hirayama, 1983; Gow, 1984; Ettema, 1986). In CRREL, the urea concentration was 1% by weight and air bubblers were used as most ice model basins do. It is noted that the air bubbles at CRREL were used not for correcting density, but for maintaining the homogeneity of growth solution over the entire tank. The urea model ice in CRREL provided scalability of up to 40 and  $E/\sigma_f$  ratio of 500-1500. In 1988, Borland (1988) study EG/AD/S model ice in a small tank at CRREL. He reported that EG/AD/S model ice had more root deflection during cantilever beam measurements in comparing to that of the urea model ice, and a filter system may be needed to prevent bacteria growth.

#### **2.1.5. Japanese experience**

Several ice tanks were built in Japan from 1981 to 1986, including IHI (the Ishikawajima-Harima Heavy Industries), MHI (the Nagasaki Research & Development Center), NKK (the Tsu Research Laboratory, NKK Corporation), and NMRI (former SRI, the National Maritime Research Institute)’s facilities (ITTC, 1999). All basins except NKK use columnar model ices with several different growth solutions, such as urea at MHI, glycol at IHI, and propylene glycol (PG) at NMRI. NKK uses a granular model ice with urea solution.

### **2.2. Granular Model ice**

#### **2.2.1. Finnish experience**

In Finland, the first ice tank was built at the Wartsila Ice Model Basin (WIMB) in 1969. Saline model ice similar to that of AARI in Russia (Enkvist, 1972) was used. In 1983, the Kvaerner-Masa Yards Arctic Research Centre (MARC) started to carry out model tests with granular model ice, called fine grain saline T1-ice or FG model ice (Enkvist and Makinen, 1984). This model ice is fundamentally different in microstructure than the columnar ice used in other model basins. The granular model ice was made by spraying saline water onto the ice to build up the ice layers. This process cuts down the ice

---

<sup>1</sup> When the ice grew, some glycol rejected from the ice into the growth solution resulted in a higher concentration of glycol deposited at the ice-water interface. Hence, more glycol could be trapped within the ice, and its strength and rigidity reduced with increased depth.

production time by half. In general, columnar model ice has a columnar structure that models the anisotropic nature of the most common type of sea ice (S2) due to the similar structure. The granular model ice, however, is isotropic.

In 1987, MARC introduced an improved version of the fine grain model ice called FGX model ice. Main difference between FG and FGX model ice was the salinity of spray water. FG model ice used 2 % saline water for tank solution and spraying, whereas FGX model ice used different salinity for spray water (0.1 - 1.6 %) and tank water (1.5 %). By controlling the salinity concentration of spray water, FGX model ice gives a better control of ice properties and production time over those of the FG model ice (Nortala-Hoikkanen, 1990).

In 1989, the Helsinki University of Technology (HUT)/ Arctic Offshore Research Centre (AORC) built its square ice tank (40 m × 40 m) (Jalonen and Ilves, 1990). HUT/AORC introduced GE (Granular Ethanol) model ice, a granular model ice that was grown from a 0.5 % ethanol solution. In 2005, the Aker Arctic Technology Inc. (AARC) started to operate with FGX model ice, but a new model ice was also planned (Wilkman et al., 2006).

The granular model ice is isotropic and homogeneous, capable of a wide range of  $E/\sigma_f$  ratio (700 - 8000) and a properly scaled density (0.88 - 0.91  $\text{Mgm}^{-3}$ ). It is cost effective due to its fast production. The major deficiency of the granular model ice is its low compressive strength (about 1-2 times flexural strength). Detailed comparison with other model ices and sea ice will be presented in Section 3. Table 1 shows the refrigerated model basins introduced in this study with built year, tank dimensions, and the model ice currently employed.

Table 1: Refrigerated model basins and their model ice

Ice Tank	Built Year	Size (L × W × D)	Model Ice, Structure
AARC	2005	75×8×2.1	FGX, Granular
AORC	1989	40×40×2.8	GE (FG-Ethanol), Granular
CRREL	1979	37×9×2.4	Urea, Columnar
HSVA	1984	78×10×2.5	Saline, Columnar
IIHR	1981	20×5×1.2	Urea, Columnar
IOT	1985	90×12×3	EG/AD/S and CD-EG/AD/S, Columnar
Krylov (KSRI)	1986	45×6×1.75	Saline & FG, Granular & Columnar
MARC (WARC)	1983-2005	77.3 × 6.5×2.3	FGX (FG until 1989), Granular
NKK	1982	20×6×1.8	FG-Urea, Granular
NMRI	1981	35×6×1.8	PG, Columnar

### 3. MECHANICAL PROPERTIES OF MODEL ICE

Weeks and Assur (1967), Wang (1979a, 1979b), Mellor (1986), Cammaert and Muggeridge (1988), and Kovacs (1996a, 1996b) have given general reviews on the mechanical properties of sea ice. The existing data on a particular physical or mechanical property of sea ice was also consolidated and analyzed, including salinity and ice thickness (Kovacs, 1996a), flexural strength (Timco and O'Brien, 1994), compressive strength (Timco and Frederking, 1990; Moslet, 2007), elastic modulus (Gagnon and Jones, 2001), and ice density (Timco and Frederking, 1996). Zufelt and Ettema (1996) reviewed model ice material.

For a proper assessment of the scalability of various model ice materials, the physical and mechanical properties of sea ice was estimated based on data obtained from the fore-mentioned reviews. The mechanical properties were computed based on a 5 parts per thousand (ppt) ice salinity and a  $-10^{\circ}\text{C}$  ice temperature. The comparison with model ice was made by using a scale ratio of 10 - 40. Brine volume is calculated by using empirical formula from Cox and Weeks (1982) and the flexural strength of sea ice (670 kPa) is estimated by formula of Timco and O'Brien (1994). Compressive strength of sea ice and freshwater ice against strain rate from Timco and Frederking (1990) and Jones (2006) is presented. Density of sea ice with pre-described conditions ranges from 0.84 to 0.925  $\text{Mgm}^{-3}$  (Timco and Frederking, 1996). The range of  $E/\sigma_f$  used is 2000 to 8000, which are needed for most model tests. Fracture toughness of sea ice used is obtained from Timco's results (Timco, 1985).

The 22<sup>nd</sup> ITTC special committee on ice established recommended procedures for the measurement of model ice properties, which included flexural strength, elastic modulus and density (ITTC, 1999). In 2002, compressive strength was included into the ITTC recommendation procedure (ITTC 7.5-02-04-02). Other properties including shear strength and fracture toughness are also important but standard methods are yet to be established. This section summarized the mechanical properties of different model ices and scaled sea ice.

#### 3.1. Flexural Strength

Flexural strength of sea ice was reviewed by Timco and O'Brien (1994). They compiled freshwater ice and sea ice data obtained from previous measurements (more than 2000 data points). The results showed that the flexural strength is a function of brine volume, and they provided empirical formula ( $\sigma_f = 1.76e^{-5.88\sqrt{v_b}}$ ). Brine volume is a function of salinity and temperature and relationship was given in Cox and Weeks (1982). The estimated flexural strength of sea ice is about 670 kPa, which is similar to the design value (690 kPa) for a recent built icebreaker "*USCGS Healy*" (Jones et al., 2001). For ice class vessels, the overall length would be between 100 and 300 meters, and the typical model length would range 5- 8 meters. Thus, the scale ratio can range from 12 to 60 and the corresponding flexural strength of model scale would be 56 kPa and 11 kPa,

respectively. It is rare that the scale ratio is over 40, so typical scale ratio and flexural strength is 10 - 40 and 15 - 60 kPa, respectively.

Regarding the dependency of flexural strength on loading direction (pull-up and push-down) for sea ice, no large difference between them was measured (Weeks and Anderson, 1958). Timco and O'Brien mentioned that the difference could be caused by a difference in grain size, but little information was available. Regarding the sensitivity of loading rate, no rate dependency was reported (Timco and O'Brien, 1994).

Since most ice failure modes during model tests, especially for ice/ship interaction, are flexural bending, the flexural strength is a primary factor to be scaled properly. In Figure 1, typical flexural strength range of model ices is shown. It is noted that the practical flexural strength should be at least 10 kPa, in order to avoid unrealistic ice failure with significant residual strength.

Although most model ices can meet the criteria of scaled flexural strength, some differences due to the difference of their microstructures exist. For granular model ice, the flexural strength shows homogeneity - the ratio of the flexural strength measured upward and downward is about 1. For columnar model ice, however, this ratio is about 0.7 for EG/AD/S ice and about 0.4 for Urea ice (Timco, 1986). CD-EG/AD/S model ice could control the homogeneity of ice strength by using air bubbles but it may cause increased residual strength. Typical ratio of CD-EG/AD/S ranges from 0.7 to near 1 depending on the thickness and tempering time.

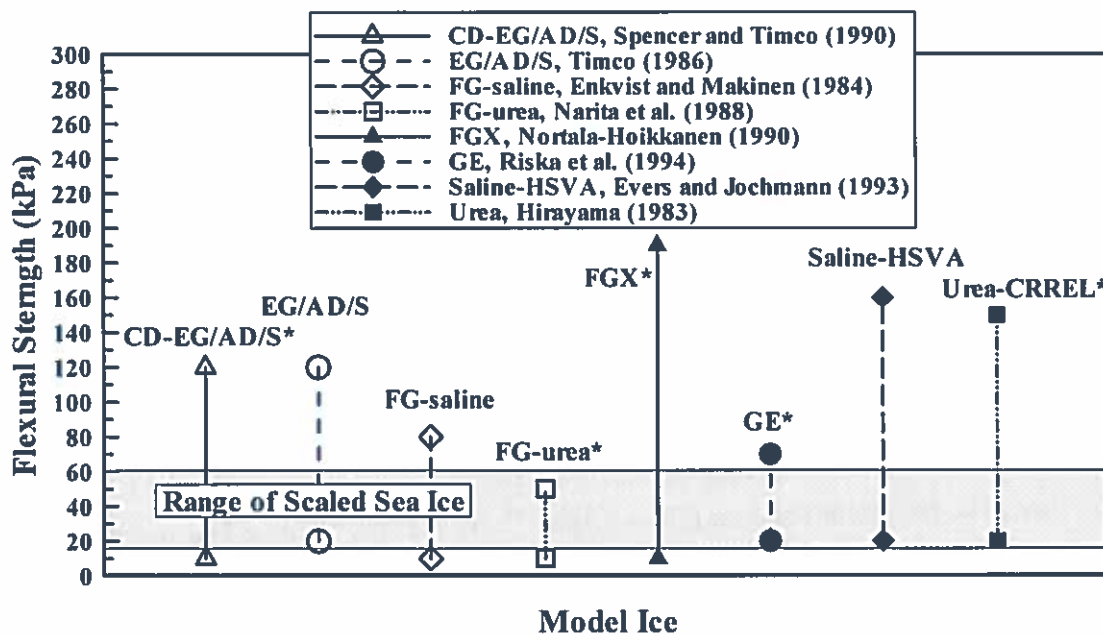


Figure 1: Typical flexural strength range of model ice (\*: best estimated)

### 3.2. Compressive Strength

USACE (2002) reviewed previous compressive tests and showed the strain rate dependency. Timco and Frederking (1990) also reviewed previous compressive tests for sea ice and developed the equations for the strain rate range of less than  $10^{-3}$ . The compressive strength is a function of porosity and strain rate, and the porosity is a function of temperature, density and salinity. Kovacs (1996b) proposed similar constitutive relationship between compressive strength and two parameters (porosity and strain rate). It is well known that sea ice is anisotropic, so that the compressive strength depends on the loading direction: for example, the vertical loading is approximately 3 times stronger than the horizontal loading (Moslet, 2007). Moslet provided the maximum strength estimated by porosity (maximum would occur at the strain rate of  $10^{-3}$ ). Compared with Timco and Frederking's results, the horizontal compressive strengths are similar (4.4 MPa from Moslet; 4.7 MPa from Timco and Frederking) but the vertical compressive strength (13.3 MPa) is about 72% of the Timco and Frederking's value (18.3 MPa). It is noted that Kovacs (1996b) reported estimation of the horizontal loaded compressive strength. In Figures 2 and 3, the compressive strength of sea ice was scaled by 30 and the data extracted from USACE (2002) is used. Since the sea ice is anisotropic, compressive strength under horizontal loading is presented.

Moore et al. (2001) presented compression test results of the CD-EG/AD/S model ice. They used a wide range of strain rates and showed the trend lines that agree well with that of sea ice over whole range of strain rate. As the sample was refrozen for testing, instead of tested in situ, i.e. floating in the tank, the strength was altered by the brine drainage and refreezing. Other model ices including EG/AD/S, FG, and FG-urea are also compared with scaled sea ice and showed the rate dependency in the limited range of strain rate (Figure 2).

In Figure 3, the relationships between flexural and compressive strengths of model ice and scaled sea ice are shown. As the compressive strength is dependent on the strain rate, the strain rate range of sea ice is assumed to be from  $10^{-3}$  to  $10^{-5}$ /s. Once it is scaled by 30, the compressive strengths corresponding to the scaled strain rate are about 110 to 40 kPa by using Timco and Frederking's equation. Therefore the ratio of  $\sigma_c/\sigma_f$  of scaled sea ice is about 1.8 to 5. In the figure, EG/AD/S shows higher values than others. It is noted that the ratio of CD-EG/AD/S has similar to EG/AD/S and it is about 2-3 times flexural strength. For FGX, the compressive strength reported is 1-2 times flexural strength (Nortala-Hoikkanen, 1990).

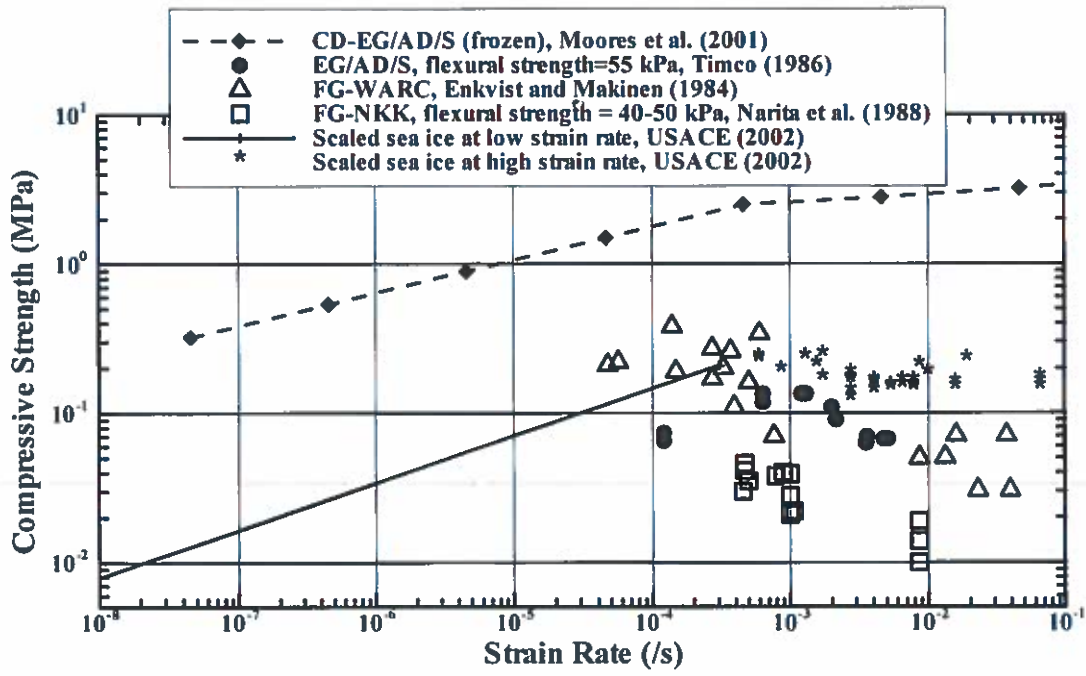


Figure 2: Compressive strength against strain rate

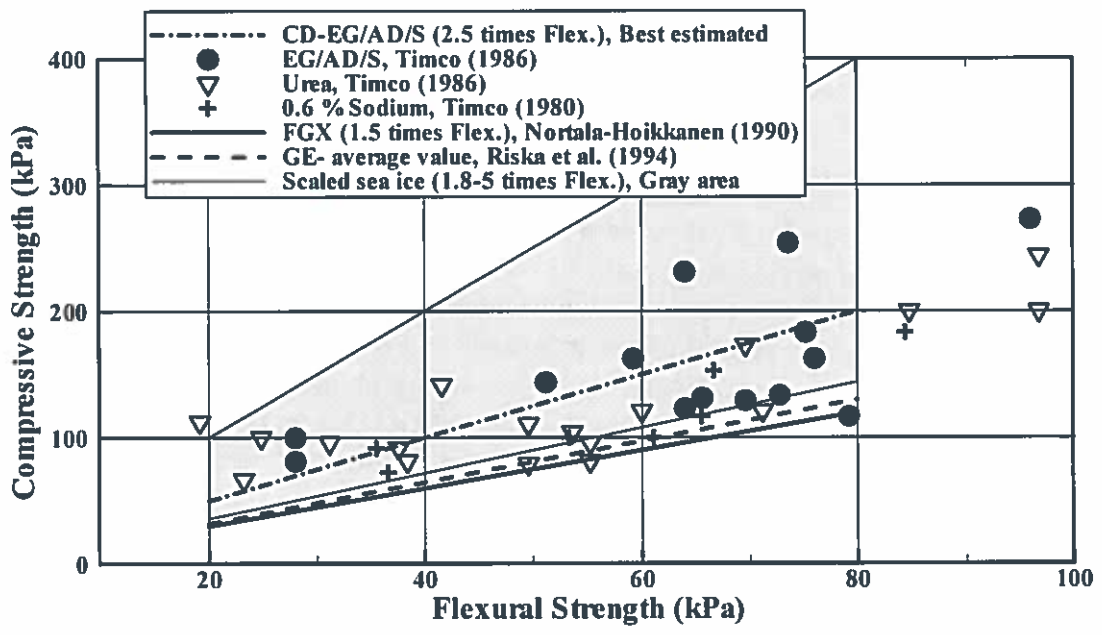


Figure 3: Compressive strength against flexural strength

### 3.3. Elastic Modulus

Elastic modulus of sea ice was studied by several investigators (Dykins, 1971; Vaudrey, 1975; Vaudrey, 1977) and reviewed by Gagnon and Jones (2001). The typical range is 3-5 GPa for salinity of 5 ppt at  $-10^{\circ}\text{C}$ . Based on the flexural strength from Timco and O'Brien (1994), the  $E/\sigma_f$  ratio of sea ice ranges from 4500 to 7500. Since the measured elastic modulus shows a wide range due to the variation of salinity, temperature, loading rate and orientation, generally  $E/\sigma_f$  ratio of 2000-8000 can be used for most model tests (Timco, 1986).

Enkvist and Makinen (1984) measured the elastic modulus of FG model ice by using two methods: beam and plate deflection methods. Elastic modulus measured from beam method was 2-5 times lower than that from plate deflection method. The ratio of  $E/\sigma_f$  for FG model ice at MARC could reach up to 2480 with 2% NaCl solution, and the typical range of  $E/\sigma_f$  ratio was between 1000 and 2000 with plate deflection method. It is noted that the plate deflection method (Sodhi et al., 1982) is a standard method to measure an elastic modulus (ITTC 7.5-02-04-02).

Timco (1986) showed that the range of elastic modulus to  $\sigma_f$  ratio for EG/AD/S was between 1500 and 2500. Introduced CD-EG/AD/S with air bubbles has elastic modulus 50 –100 % greater than that of normal EG/AD/S (Spencer and Timco, 1990). From the experience at IOT, the average  $E/\sigma_f$  ratio for CD-EG/AD/S can range from 2000 – 3100. For the solution of 0.9% sodium chloride with air bubbles and ice scraper (used at HSVA), the typical values of  $E/\sigma_f$  ratio, elastic modulus and flexural strength were 4000, 160 MPa and 40 kPa, respectively (Evers and Jochmann, 1993).

Narita et al. (1988) at NKK showed that the range of the  $E/\sigma_f$  ratio was 200 to 310 from urea granular model ice. Riska et al. (1994) reported that the GE (Granular Ethanol) model ice had a good agreement with scaled sea ices. The elastic modulus of FGX is not shown in Figure 4 due to lack of data points, but the ratio of  $E/\sigma_f$  reported could be four times of that of FG and ranging from 700 to 8000 (Nortala-Hoikkanen, 1990). This range reported above is somewhat wide, because it depends on the salinity of spraying water (0.1 – 1.6 %).

Comparisons of model ices and sea ice for the elastic modulus are made in Figure 4. CD-EG/AD/S, FGX, GE and saline (HSVA) model ices can meet the range of sea ice.

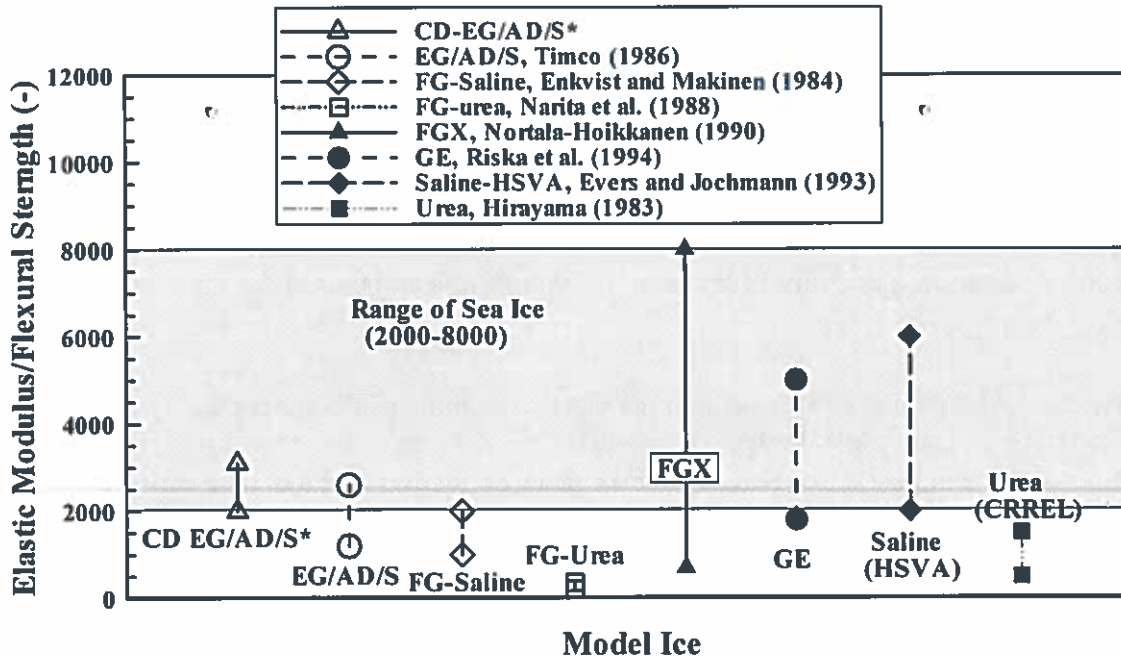


Figure 4: Elastic modulus vs. flexural strength (\*: best estimated)

### 3.4. Fracture Toughness

The fracture toughness for sea ice was investigated by Urabe et al. (1980), Timco and Frederking (1982), Urabe and Yoshitake (1984), Timco (1985), and Parsons et al. (1986). They found that the fracture toughness depends on the strain rate (when it is more than  $10^{-3}$  /s), brine volume, grain size and orientation. Generally, at strain rate which is lower than  $10^{-3}$  /s, the fracture toughness is constant, and when the strain rate is higher than  $10^{-3}$  /s, the fracture toughness decreases. Larger brine volume and smaller grain size decreases the fracture toughness. Data for scaled sea ice is used from Timco's estimations (Timco, 1985). Measurement of fracture toughness as part of model ice characterization was suggested by Parsons and Snellen (1985) and Parsons et al. (1988).

The comparison of fracture toughness from model ice and sea ice is shown in Figure 5. For EG/AD/S and CD-EG/AD/S model ices, the fracture toughness was measured and reported by Timco (1986) and Spencer and Timco (1990), respectively. Spencer and Timco explained that CD-EG/AD/S model ice could reduce the ratio of the fracture toughness to downward breaking strength by strengthening the top layer with air bubbles at target flexural strength. The comparison, however, shows normal EG/AD/S is somewhat better than CD-EG/AD/S. For FG model ice, fracture toughness was somewhat higher than that of EG/AD/S and GE model ice. The GE model ice shows the similar fracture toughness values to the EG/AD/S, but the data is limited for low flexural strength only.

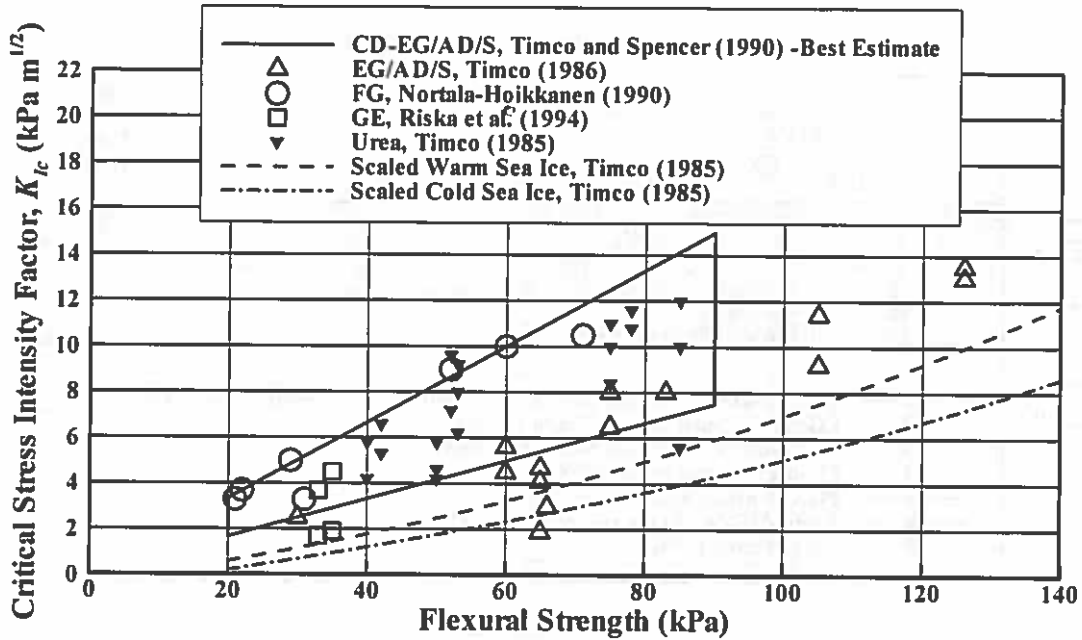


Figure 5: Critical stress intensity factor vs. flexural strength

### 3.5. Density

Density of sea ice was reviewed by Timco and Frederking (1996). They used a number of previous density measurements for first year and multi-year ices. They reported that the density range of sea ice was from 0.72 - 0.94  $\text{Mgm}^{-3}$ . This wide range is because the sea ice is composed of solids, liquids, and gas and the density depends on their amount. The density is also sensitive to temperature. For the first year ice, the values range from 0.84 to 0.91  $\text{Mgm}^{-3}$  for the upper part (above the waterline), and the lower part (below the waterline) density ranges from 0.9 to 0.94  $\text{Mgm}^{-3}$ . For comparison, density for salinity of 5 ppt at 10°C would have an upper limit of about 0.925 (for gas free sea ice). It is noted that as the salinity or brine volume increases, the density increases.

Early columnar model ice had somewhat higher density compared to the sea ice, as mentioned earlier. For EG/AD/S, the density range was from about 0.94 to 0.98  $\text{Mgm}^{-3}$ . For CD-EG/AD/S model ice (Spencer and Timco, 1990), the density range was varied between 0.86 and 0.91  $\text{Mgm}^{-3}$  by using air bubbles. Spencer and Timco mentioned that the density could be controlled below 0.8  $\text{Mgm}^{-3}$ , but the compressive properties could be changed. HSVAs saline model ice can control the density with air bubbles. Density from various model ices and sea ice is compared in Figure 6.

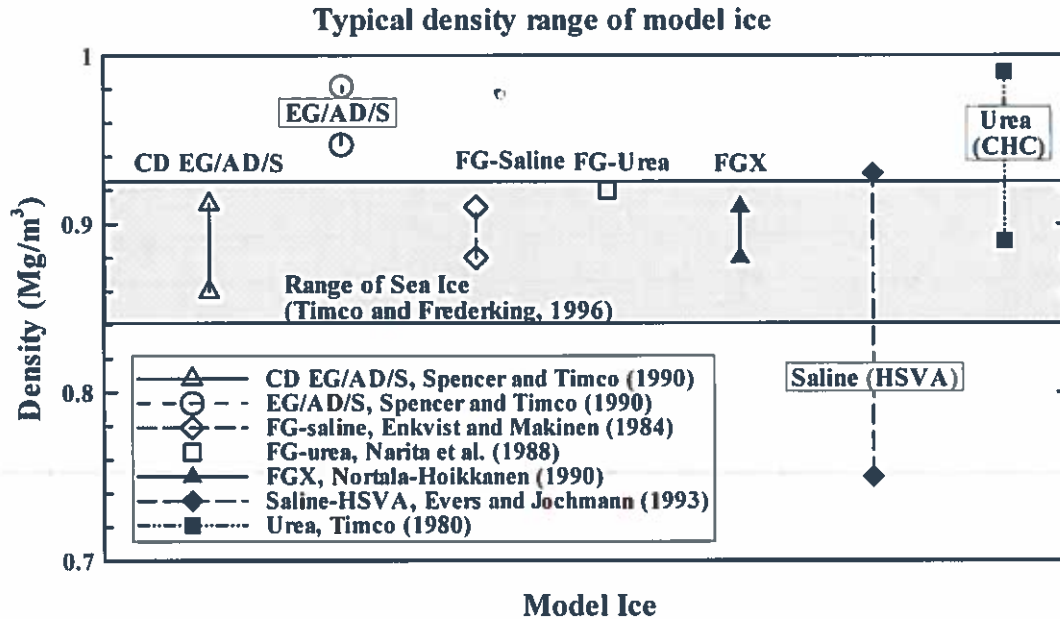


Figure 6: Typical density range of model and sea ice

### 3.6. Summary of Mechanical Properties of Model Ice

The mechanical properties of existing model ices were compared with those of sea ice. As shown in this section, most model ices meet the flexural strength criteria for scaled sea ice that has a salinity of 5 ppt and temperature of  $-10^{\circ}\text{C}$ . Experimental results for compressive strength against strain rate are very limited, but model ices including EG/AD/S, CD-EG/AD/S, FG, FG-saline shows a strain rate dependency. For  $E/\sigma_f$  ratio, CD-EG/AD/S, FGX, GE and saline (HSVA) model ices can meet the proper range for sea ice. The fracture toughness of most model ices is somewhat greater than that required of model ice. Most granular ices have a good density range. Once air bubbles are used for columnar ice, the density range can achieve that of sea ice. In general, columnar model ices need air bubble and/or ice scraper systems to achieve required model ice properties. For granular ice, different salinity or dopant of tank/spraying water can help to control the ice properties.

Although it was reported that EG/AD/S model was superior to urea model ice in all aspects, an appropriate concentration of EG, AD and S is crucial. Several ice tanks have tried the EG/AD/S solution but the scalability of EG/AD/S model ice is very sensitive to the proportions of the dopants. The cost of glycol is about 4 times of urea; however, the glycol is more durable and economical in the long run, as the urea solution needs to be changed regularly or the mechanical properties change with time. By comparison mechanical properties of EG/AD/S ice are stable over many years. For saline model ice, the ice tank and facilities need to be designed to resist the corrosive effects of salt. With

regard to the ice structure, sea ice has columnar structure (Lainey and Tinawi, 1984), so the model ice should also be able to model the anisotropical behavior due to its structure.

#### 4. SCALING

Confidence in the scalability of model ice and the interaction processes during ice-structure or ice-ships interactions is key to the prediction of full-scale behaviour from model test measurements. Timco (1984) has presented the theoretical basis of the scaling law. Timco categorized physical modeling for ice tests into two cases: flexural failure dominant for ship or inclined structure-ice interaction case and crushing failure dominant case for dynamic interaction. Derivation of scaling laws for model tests in ice has been studied by several investigators (White and Vance, 1967; Atkins and Caddell, 1974; Atkins, 1975; Michel, 1978; and Timco, 1984). Generally, they were focused on the Froude scaling that was applicable for most model tests in ice. In this section a brief summary of the scaling laws is given.

For a complete similitude, the geometric, kinematic, and dynamic similitude must be maintained. In most cases, model Froude and Reynold Numbers cannot be preserved at the same time with normal working fluids. In most model tests, where flexural failures predominate such as ship resistance, correct scaling of the gravity and inertial forces is important. Froude Number is a ratio of inertial to gravitational forces as shown below.

$$F_r = \frac{V}{\sqrt{gL}} = \frac{\textit{inertia forces}}{\textit{gravitational forces}}$$

where  $V$  is the representative velocity,  $g$  is the gravitational acceleration, and  $L$  is the representative length.

In practice, the model ice is scaled according to Froude and Cauchy scaling with the scaling of Reynold Number ignored. The Cauchy scaling is necessary to model the elastic behaviour in ice deformation, i.e., properly scaling of ice deflection and characteristic length. Cauchy Number is a ratio of inertia to elastic force as shown below.

$$C_n = \frac{\rho V^2}{E} = \frac{\textit{inertia forces}}{\textit{elastic forces}}$$

where  $V$  is the representative velocity,  $\rho$  is the density, and  $E$  is the elastic modulus.

With regard to fracture toughness, Aktins (1975) introduced an “Ice Number ( $I_n$ )” to ensure the ratio of ice-cracking forces to inertial forces is preserved at model scale. Ice Number is a ratio of Cauchy Number to fracture toughness as shown below.

$$I_n = C_n^2 \left[ \frac{EL}{R} \right]^{1/2}$$

where  $C_n$  is the Cauchy Number,  $E$  is the elastic modulus,  $L$  is the characteristic length, and  $R$  is the fracture toughness.

The fracture toughness similitude may be crucial for certain types of tests, but a number of issues for scaling the toughness, including standardized measuring standard for fracture toughness characterization in model scale have discouraged the scaling of this property (ITTC, 1999). The scaling laws are summarized in Table 2.

Table 2: Summary of scaling laws according to Froude and Cauchy scaling (Timco, 1984)

Variable	Scaling
ice thickness	$[h]_p = \lambda [h]_M$
ice compressive strength	$[\sigma_c]_p = \lambda [\sigma_c]_M$
ice flexural strength	$[\sigma_f]_p = \lambda [\sigma_f]_M$
ice shear strength	$[\sigma_s]_p = \lambda [\sigma_s]_M$
ice elastic modulus	$[E]_p = \lambda [E]_M$
velocity	$[V]_p = \lambda^{1/2} [V]_M$
time	$[T]_p = \lambda^{1/2} [T]_M$
force	$[F]_p = \lambda^3 [F]_M$
mass	$[M]_p = \lambda^3 [M]_M$
ice critical stress intensity factor	$[K_{Ic}]_p = \lambda^{3/2} [K_{Ic}]_M$
acceleration	$[a]_p = [a]_M$
the ratio of elastic modulus and flexural strength	$[E/\sigma_f]_p = [E/\sigma_f]_M$
ice frictional coefficient	$[f]_p = [f]_M$
ice density	$[\rho]_p = [\rho]_M$
Poisson ratio	$[\nu]_p = [\nu]_M$

Note: Subscripts P and M refer to prototype and model respectively.

## 5. TEST METHODOLOGY AND DATA ANALYSIS FOR SHIP IN ICE PERFORMANCE EVALUATIONS

Ship resistance, propulsion, and maneuvering are three major performance evaluation tests. These tests and the associated data analysis are described in this section.

### 5.1. Ship Resistance in Ice

Ship transiting in ice involves several different physical processes including ice breaking, ice submerging, ice clearing, and open water resistance. The total force on the ship can be delineated into different components assuming these force components can be superpositioned to estimate the total force. The individual force component can be derived by considering relevant ice mechanics theories and experimental data associated with respective processes. For example, ice strength is the most important influencing factor on ice breaking, but ice density and friction are important factors affecting ice submerging and clearing. It is possible to estimate each component by considering the influence of relevant factors through dimensional analysis and the underlying physical process. The breakdown of these components was initially suggested by Kashteljan et al. (1968) by using four components:

$$R = R_1 + R_2 + R_3 + R_4$$

where  $R$  is the total resistance in ice,  $R_1$  is the resistance due to breaking ice,  $R_2$  is the resistance due to buoyancy and friction,  $R_3$  is the resistance due to penetration through broken ice, and  $R_4$  is the open water resistance. The equation for each component is given as follows:

$$\begin{aligned}R_1 &= k_1 B \sigma_p h \mu_o \\R_2 &= k_2 \gamma_\lambda B h^2 \mu_o \\R_3 &= k_3 B^x h v^y \frac{1}{\eta_2}\end{aligned}$$

where  $B$  is the beam of the icebreaker,  $\sigma_p$  is the critical bending stress,  $h$  is the ice thickness,  $\mu_o$  is the efficiency factor (1+ the ratio of total horizontal stresses to vertical stress),  $\gamma_\lambda$  is the specific weight of ice,  $\eta_2$  is the ice-cutting coefficient (the ratio of total transverse stress to the total longitudinal stress),  $v$  is the vessel speed, and  $x, y, k_1, k_2, k_3$  are empirical factors.

Lewis and Edwards (1970) suggested a component breakdown of the ice resistance for continuous icebreaking as shown below:

$$R_{im} = C_o \sigma h^2 + C_1 \rho_i g h^2 + C_2 \rho_i B h v^2$$

where  $R_{im}$  is the mean resistance in ice without open water resistance,  $\sigma$  is the flexural ice strength,  $h$  is the ice thickness,  $\rho_i$  is the ice density,  $B$  is the beam of the vessel,  $g$  is the gravitational acceleration, and  $C_o, C_1, C_2$  are empirical factors.

Enkvist (1972) shows a similar functional form of the resistance equation applicable to continuous ice breaking:

$$R_i = R_\sigma + R_S + R_V$$

where  $R_i$  is the total resistance in ice,  $R_\sigma$  is the resistance due to breaking,  $R_S$  is the resistance due to the submersing, and  $R_V$  is the resistance due to the velocity effects. He also showed the non-dimensional form for each component as below:

$$R_\sigma = C_C B h \sigma$$

$$R_S = C_S B h T \rho_d g$$

$$R_V = C_V B h \rho_i V^2$$

where  $B$  is the beam of the vessel,  $h$  is the ice thickness,  $\sigma$  is the flexural ice strength,  $\rho_d$  is the density difference between water and ice,  $g$  is the gravitational acceleration,  $V$  is the vessel speed, and  $C_C, C_S, C_V$  are empirical factors.

Ponanjak and Ionov (1981) presented three basic terms (breaking, submerging, and velocity) and a friction term associated with each basic term.

$$R_T = R_\sigma + R_{f\sigma} + R_S + R_{fS} + R_V + R_{fV}$$

It may be important to use different frictional factors for different icebreaking process.

Enkvist (1983) presented the relationship between the submersion and breaking components of ice resistance. Model tests and full scale tests were carried out by using pre-sawn ice and the results showed that the breaking resistance is about 40-80 % of total zero speed resistance. It is noted that the velocity dependent component was not considered.

Colbourne and Lever (1992) developed further the component analysis methodology. They developed the testing procedure to isolate the individual force components by performing model test in level ice, pre-sawn ice and open water. This method has been adopted by other tanks. The total resistance from this method is divided by three components: icebreaking resistance ( $R_B$ ), ice clearing resistance ( $R_C$ ), and viscous drag resistance ( $R_V$ ).

They showed the non-dimensional term of each component in order to derive the scaling parameter as shown below:

$$C_B = \frac{R_B}{\rho_i B h V^2} = \Phi_B(S_N)$$

$$C_C = \frac{F_C}{\rho_i B h V^2} = \Phi_C(Fr)$$

$$C_V = \frac{R_V}{0.5 \rho_w S V^2} = \Phi_V(Re)$$

where  $B$  is the beam of the ship,  $h$  is the ice thickness,  $V$  is the ship speed,  $S_N$  is Strength Number ( $\frac{V}{\sqrt{\sigma / \rho_i}}$ ),  $Fr$  is the Froude Number, and  $Re$  is the Reynold's

Number. In practice, viscous drag is calculated using ITTC method or from open water resistance test, and the other two terms are determined by level ice and pre-sawn ice tests. The breaking resistance can be determined by subtracting the resistance in presawn ice from level ice resistance.

Riska et al. (1994) introduced another equation for analyzing resistance test data, which is similar to previous equations proposed by Lewis and Edwards (1970) and Enkvist (1972, 1983). Their equation consisted of four components:

$$R = R_B + R_S + R_V + R_{HW}$$

where  $R_B$  is the resistance due to icebreaking,  $R_S$  is the resistance due to ice submersion,  $R_V$  is the resistance due to velocity dependent resistance, and  $R_{HW}$  is the hydrodynamic resistance in the presence of ice.

In order to correct the test results due to the discrepancy of ice properties during the tests from target values, the measured resistance can be modified with the ice thickness and strength as below (Riska et al., 1994).

$$R_I = \left( R_B \left( \frac{\sigma_{f(Target)}}{\sigma_{f(Measured)}} \right) + R_S + R_V \right) \left( \frac{h_{I(Target)}}{h_{I(Measured)}} \right)^x$$

where  $\sigma_f$  is the flexural strength,  $h_i$  is the thickness of the model ice, and  $x$  ranges from 1.5 to 2 depending on the hull shape. Therefore, full scale net ice resistance can be calculated from  $R_{IP} = \lambda^3 R_{IM}$  or  $R_{IP} = C_\mu \lambda^3 R_{IM}$  if friction correction is needed ( $C_\mu$  is an empirical friction correction factor).

### 5.1.1. ITTC standard method

ITTC (1996) proposed the standard test method for ship resistance tests in ice. The procedures are very similar to that of Riska et al. (1994), but ITTC does not include the submersion resistance term ( $R_s$ ). Therefore net ice resistance ( $R_I$ ) is sum of the breaking component ( $R_B$ ) and the speed dependent component ( $R_V$ ). Breaking component can be separated from net ice resistance by using pre-sawn ice. The breath of the pre-sawn area may be calculated by the sum of the breath of waterline model and 3-4 times ice thickness. Usually, level ice should be prepared at least two times ship length for the resistance tests. For the effect of variation from ice thickness and strength on the resistance, the correction of resistance is shown below:

$$R_I = \left( R_{V(Measured)} + R_{B(Measured)} \frac{\sigma_f}{\sigma_{f(Measured)}} \right) \left( \frac{h_i}{h_{I(Measured)}} \right)^x$$

For correction, simple ice thickness correction and both ice thickness and strength correction are also considered as  $R_I \approx h_i^{1.5}$  and  $R_I = a(v)\sigma_f h_i^2 + b(v)\sigma_f h_i$ , respectively, where  $a$  and  $b$  are constants, and  $v$  is the model speed. Correction for friction can be used, which is similar to that of Riska et al. (1994).

### 5.1.2. IOT standard method

Spencer and Jones (2001) have further developed the component method based on analysis of resistance data accumulated in IOT's model test database. They introduced a standard four components analysis procedure (Jones et al. 1994; IOT, 2000) for analyzing ice resistance. This procedure has been adopted by most ice tanks. They showed the total resistance in ice is:

$$R_T = R_{BR} + R_C + R_B + R_{OW}$$

where  $R_T$  is the total resistance in ice,  $R_{BR}$  is the resistance due to icebreaking,  $R_C$  is the resistance due to ice clearing,  $R_B$  is the resistance due to ice buoyancy, and  $R_{OW}$  is the resistance due to open water.

For estimating the icebreaking resistance, level ice and pre-sawn ice tests are needed (subtracting the pre-sawn ice resistance from level ice resistance) as shown below:

$$R_{BR} = R_T - R_{PS}$$

where  $R_{PS}$  is the resistance in pre-sawn ice.

Because the pre-sawn ice resistance includes the hydrodynamic loads from open water resistance tests, sum of two resistances ( $R_C + R_B$ ) is calculated by subtracting open water resistance from pre-sawn ice resistance:

$$R_C + R_B = R_{PS} - R_{OW}$$

The buoyancy resistance can be determined by performing test with very low speed ( $V=0.02$  m/s) in pre-sawn ice, which eliminates the dynamic (velocity dependent) forces such as ice block rotation, ventilation, and acceleration. The clearing resistance ( $R_C$ ), which is velocity dependent, can be calculated by subtracting the buoyancy resistance ( $R_B$ ) from  $R_C + R_B$ .

Spencer and Jones (2001) presented non-dimensional form of each component by considering their relevant influencing factors. This gave a non-dimensional coefficient for each individual component. The coefficient for the breaking resistance was a function of ice density ( $\rho_i$ ), ship/model beam ( $B$ ), ice thickness ( $h$ ), and ship/model speed ( $V_m$ ):

$$C_{BR} = \frac{R_{BR}}{\rho_i B h V_m}$$

Similarly, the coefficient for the clearing resistance was:

$$C_C = \frac{R_C}{\rho_i B h V_m}$$

For the coefficient of the buoyancy resistance, density difference and maximum draft of the model are included.

$$C_B = \frac{R_B}{\Delta\rho_i g B h T_m}$$

where  $\Delta\rho_i$  is the density difference between ice and water,  $g$  is the gravitational acceleration, and  $T_m$  is the maximum draft of the model. Spencer and Jones provided two additional non-dimensional parameters, which are the Strength Number ( $S_N = \frac{V_M}{\sqrt{\frac{\sigma_f h_i}{\rho_i B}}}$ )

and the Froude Number ( $F_h = \frac{V_m}{\sqrt{g h_i}}$ ). The breaking resistance and clearing resistance coefficients are dependent on the Strength Number and Froude Number, respectively, which are similar to those of Colbourne and Lever (1992).

The afore-mentioned resistance equations are similar in form, with three or four components to model respective interaction processes. Some differences can be found when the data is analyzed: for example, using the correction method or the non-dimensional method. The correction method from Riska et al. (1994) and ITTC (1996) may be necessary for compensating the deviation of ice flexural strength and thickness from target values. This method, however, needs a number of data sets in order to relate the resistance to ice thickness and flexural strength. The non-dimensional method would be convenient because dimensionless coefficients present the results at given conditions and erroneous data points can be easily identified.

## **5.2. Propulsion in Ice**

The purposes of propulsion tests in ice are to assess the required propulsion power in ice conditions, the propulsive coefficients, the ice interaction with appendages and propulsion system, and the optimized stern configuration (ITTC, 1996). The propulsion tests are carried out with a free running test or captive model test (towed propulsion tests). In the free running test, the propeller speed is fixed and the model velocity is measured at steady condition. In the captive model test, two to three different propeller speeds are used at the same carriage speed, and then the test data are interpolated to zero pull to determine the self propulsion point.

The propulsion performance can be evaluated by conducting resistance and self-propulsion tests in ice conditions. The self-propulsion tests generally show a large variation of results due to the physical interaction between propeller and ice. Once the propeller-ice interaction occurs, the measured thrust and torque are significantly changed, and the measurement of wake fraction and constant values of thrust deduction fraction at a certain ice condition are almost impossible to determine due to the presence of the ice and the interaction with the ice, respectively.

Since the 22<sup>nd</sup> ITTC ice committee suggested that the standard method for propulsion in ice (ITTC 7.5-02-04-02.2) needs substantial revision before being acceptable, test methodology employed by IOT is presented here.

### **5.2.1. IOT method**

Molyneux (1989) introduced the overload test technique for propulsion tests in ice. The principle of this method is to estimate the hydrodynamic torque for ice-covered water by using overload tests in open water. In order to identify the increased torque during propeller-ice interaction, the same tests in ice should be carried out. The ice effect on the thrust is assumed to be negligible for small values of  $h_i / D$ , where  $h_i$  is the ice thickness and  $D$  is the propeller diameter. Since this method can consider hydrodynamic and ice loads separately, assessment of the propulsion performance can be evaluated from open water tests and the ice loads can be added. Another advantage to this method is that the overload propulsion tests can be carried out during the resistance tests in ice if the propellers are easily removed or installed. This overload method has been adapted for

most propulsion tests in ice at IOT (Jones et al., 1994; Spencer and Jones, 2001; Jones and Lau, 2006). In order to determine the delivery power of the propulsion system without propeller-ice interaction, the procedure is shown below:

1. Carry out overload tests in open water in order to equate the tow force/torque and rps for a given speed
2. Determine the ice resistance at given ice thickness, ice strength, and given speed from Step 1.
3. Determine the rps for measured tow force in ice (Step 2) from the overload tests results (Step 1).
4. Determine torque value from measured torque value in ice (Step 2) from the overload tests results (Step 1).
5. Calculate the delivery power ( $P_D = 2\pi nQ$  where  $n$  is the rps and  $Q$  is the torque in open water) in ice.

When the propeller-ice interaction occurs,

6. Calculate the ratio of torque in ice ( $Q_i$ ) to that in open water ( $Q$ ) and multiply  $P_D$  (Step 5) by the ratio ( $Q_i/Q$ ) for given speed and ice condition. The ratio of thrust in ice ( $T_i$ ) to that in open water ( $T$ ) is also determined in order to compare to the open water values.

### 5.3. Maneuvering in Ice

The purpose of maneuvering tests in ice is to assess the effectiveness of the hull and turning devices (rudders, thrusters, or azimuthing propulsors) when the vessel turns in ice. Typical maneuvering tests in ice are turning circle tests, star maneuvers and breaking out of channel (ITTC 7.5-02-04-02.3). The ITTC procedure does not include the PMM (Planar Motion Mechanism) testing and the 22<sup>nd</sup> ITTC ice committee suggested that substantial change may be needed. Therefore, several maneuvering model tests, which have been carried out at IOT, are introduced here and discussed.

In order to assess the ship maneuverability in ice, two test methods are considered, which are free-running model tests and captive model tests. Both test procedures may be similar to that for open water, but ice tests are more complex to carry out due to the variation of ice properties and ice failure. Shi (2002) reviewed the test method and presented the data analysis for maneuvering tests in ice tank.

#### 5.3.1. Free running model tests

The main advantage of this test is to simulate the full-scale trials visually and to assess all aspects of the flow and resulting forces accurately. It may be more complex than captive model test because the interaction between ice and the hull of the model may not reach steady state. Sometimes, predicted self-propulsion point for certain speed would not be

enough to carry out the test due to the additional skin friction at model scale (Spencer and Williams, 1998). At IOT, Molyneux et al. (1998) carried out the free running model tests with two model icebreakers, R-Class and M/V Arctic.

The procedure to conduct the free running model test in ice is:

1. Set the shaft speed
2. Allow the model to accelerate until it reaches steady-state
3. Deflect the rudder angle at desired degree
4. Measure the shaft speed, rudder angle, yaw rate, thrust and torque of the propeller, and model speed and position

### **5.3.2. Captive model tests**

Most ice model basins have rectangular shape and generally not enough width to carry out the free running model tests. Most captive model tests are carried out with a planar motion mechanism (PMM) or a rotating arm. From these tests, most coefficients (or derivatives) for equation of motion can be determined. The unique feature of the PMM is that it provides the sinusoidal yawing and swaying motion when the model is towed. The Institute for Ocean Technology (IOT) has performed a large number of model tests using its PMM (Marineering Limited, 1997; Williams and Waclawek, 1998; and Lau and Derradji-Aouat, 2004).

Due to the limitation of tank size for 1:20 scale model at the speed of 1.2 m/s, full steady state arc tests instead of full turning were carried out (Lau and Derradji-Aouat, 2004). The arc should be at the steady state and the length of the arc should be at least 2 times model length. In order to avoid edge effect, the distance between consecutive arcs should be 3 times characteristic length. From the constant radius arc, pure sway and pure yaw tests, complete information for the motion is obtained.

#### Typical Set-Up

The model is rigidly attached to the PMM, which is rigidly attached to the ice tank carriage. The carriage controls the model's surge motion, and the PMM controls the model's yaw and sway motions, so to produce a desired planer motion. The model's heave and pitch motions are unrestricted. The basic premise of PMM testing is that the hydrodynamic and ice derivatives (as described in the following sub-section) governing the manoeuvring performance of a vessel can be determined by forcing the model to perform predetermined prescribed motions and recording the resulting forces and moments (Marineering Limited, 1997). Vessel manoeuvring characteristics can then be predicted.

#### Equations of Motion

The general manoeuvring equations governing the motions of a vessel are given as follows:

$$-Y'_v v' - (m' - Y'_\xi) \xi - (Y'_r - m') r' - (Y'_\xi - m' x'_G) \xi = Y'_\delta \delta$$

$$-N'_v v' - (N'_\xi - m' x'_G) \xi - (N'_r - m' x'_G) r' + (I'_z - N'_\xi) \xi = N'_\delta \delta$$

where:

$m' = \frac{m}{\frac{\rho}{2} L^2 T}$	Non-dimensional ship mass
$I'_z = \frac{I_z}{\frac{\rho}{2} L^4 T^2}$	Non-dimensional ship heave mass moment of inertia
$v' = \frac{v}{V}$	Non-dimensional ship sway velocity
$\xi = \frac{\xi}{V}$	Non-dimensional ship sway acceleration
$r' = \frac{rL}{V}$	Non-dimensional ship yaw rate
$\xi = \frac{\xi^2}{V^2}$	Non-dimensional ship yaw acceleration
$\delta' = \delta$	Non-dimensional ship rudder angle
$Y'_v = \frac{Y_v}{\frac{\rho}{2} LTV}$	Non-dimensional derivative of $Y$ due to $v$
$N'_v = \frac{N_v}{\frac{\rho}{2} L^2 TV}$	Non-dimensional derivative of $N$ due to $v$
$Y'_\xi = \frac{Y_\xi}{\frac{\rho}{2} L^2 T}$	Non-dimensional derivative of $Y$ due to $\xi$
$N'_\xi = \frac{N_\xi}{\frac{\rho}{2} L^3 T}$	Non-dimensional derivative of $N$ due to $\xi$
$Y'_r = \frac{Y_r}{\frac{\rho}{2} L^2 TV}$	Non-dimensional derivative of $Y$ due to $r$
$N'_r = \frac{N_r}{\frac{\rho}{2} L^3 TV}$	Non-dimensional derivative of $N$ due to $r$

<sup>2</sup> Marineering Limited, 1997, P 14 reported this as  $I'_z = \frac{I_z}{\frac{\rho}{2} L^3 T}$  which is not non-dimensional.

$$Y_{\&} = \frac{Y_{\&}}{\frac{\rho}{2} L^3 T} \quad \text{Non-dimensional derivative of } Y \text{ due to } \&$$

$$N'_{\&} = \frac{N_{\&}}{\frac{\rho}{2} L^4 T} \quad \text{Non-dimensional derivative of } N \text{ due to } \&$$

$$Y'_{\delta} = \frac{Y_{\delta}}{\frac{\rho}{2} L T V^2} \quad \text{Non-dimensional derivative of } Y \text{ due to } \delta$$

$$N'_{\delta} = \frac{N_{\delta}}{\frac{\rho}{2} L^2 T V^2} \quad \text{Non-dimensional derivative of } N \text{ due to } \delta$$

$m$  Ship mass

$I_z$  Ship heave mass moment of inertia

$v$  Sway velocity (lateral speed) [m/s]

$\&$  Sway acceleration (lateral acceleration) [m/s<sup>2</sup>]

$r$  Yaw rate [rad/s]

$\&$  Yaw acceleration [rad/s<sup>2</sup>]

$x_G$  Position of centre of gravity [m]

$I_z$  Yaw moment of inertia [kg-m<sup>2</sup>]

$\delta$  Rudder angle [degrees]

$\rho$  Mass density of water [kg/m<sup>3</sup>]

$L$  Ship length (L<sub>WL</sub>) [m]

$T$  Ship draft [m]

$V$  Ship speed (forward) [m/s]

$Y_v$  Derivative of sway force due to sway velocity [kg/s]

$N_v$  Derivative of yaw moment due to sway velocity [kg-m/s]

$Y_{\&}$  Derivative of sway force due to sway acceleration [kg]

$N_{\&}$  Derivative of yaw moment due to sway acceleration [kg-m]

$Y_{\delta}$  Derivative of sway force due to rudder angle [kg-m/s<sup>2</sup>]

$N_{\delta}$  Derivative of yaw moment due to rudder angle [kg-m<sup>2</sup>/s<sup>2</sup>]

$Y_r$  Derivative of sway force due to yaw rate [kg-m/s]

$N_r$  Derivative of yaw moment due to yaw rate [kg-m<sup>2</sup>/s]

$Y_{\&}$  Derivative of sway force due to yaw acceleration [kg-m]

$N_{\&}$  Derivative of yaw moment due to yaw acceleration [kg-m<sup>2</sup>]

These equations of motion have been derived for model ship manoeuvring in ice based on a series of assumptions (Marineering Limited, 1997):

- Higher order derivatives are ignored, but can be easily included if necessary.

- The model's centre of gravity is assumed to be on the model's centreline; therefore  $y_G$  (distance to lateral centre of gravity from model's centreline) is assumed to be zero.
- The model is assumed to be symmetrical along the centreline so that  $Y_u$  and  $Y'_u$  are assumed to be zero.

### Types of PMM Maneuvres

The different types of controlled manoeuvres are summarized in Figure 7.

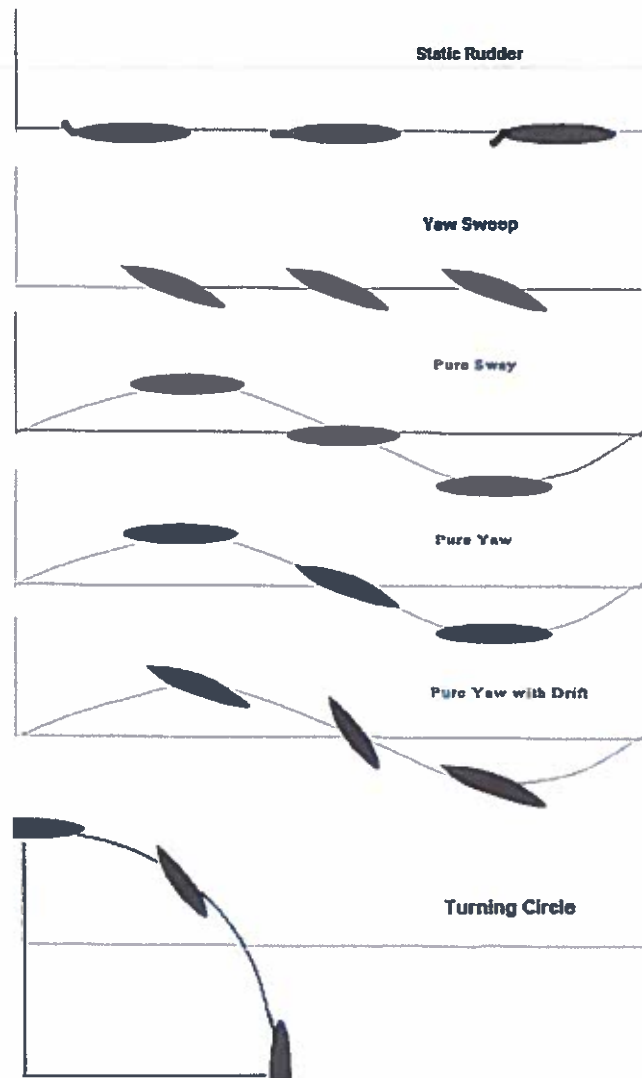


Figure 7: Standard PMM tests (modified from Marineering Limited, 1997)

### Static Rudder Tests

The model is fixed straight ahead and the rudder is moved from hard port to hard starboard in discrete increments as the model is towed down the tank at its self-propulsion speed (to ensure proper flow around the stern). The ice derivatives,  $X_\delta$ ,  $Y_\delta$ , and  $N_\delta$  are found by plotting  $X$ ,  $Y$ , and  $N$ , respectively, versus  $\delta$ . If the plots are highly non-linear, a higher order fit should be applied and the above equations of motion modified. The effect of ship speed can be determined by performing these tests for a range of speeds.

### Yaw Sweep Tests

Yaw sweep tests are performed by fixing the model at a drift angle,  $\beta$  (about the vertical axis), to the direction of motion. This induces a lateral flow component on the hull described by  $v = -V \sin \beta$ , where  $V$  = Ship's forward speed (m/s),  $v$  = Lateral speed [m/s], and  $\beta$  = drift angle. A plot of  $X$ ,  $Y$ , and  $N$  versus  $v$  yields  $Y_v$  and  $N_v$  (also found from pure sway tests).

### Pure Sway Tests

The pure sway test is performed by fixing the model's heading (e.g.  $\beta=0$ ) and moving the carriage down the tank at a fixed speed while swaying the model in a sinusoidal pattern of amplitude,  $Y_o$ , and period,  $\tau$ . This motion produces a variable lateral cross flow and the resulting forces and moments are due to the model's velocity and acceleration. This motion can be parametrically described by:

$$\begin{aligned}x &= Vt \\y &= Y_o \cos \omega t \\ \phi &= 0 \\ \omega &= \frac{2\pi}{\tau}\end{aligned}$$

Where:  $x$  = surge position

$y$  = sway position

$Y_o$  = sway amplitude

$\omega$  = circular frequency

$t$  = time

$\phi$  = yaw angle

$\tau$  = period of oscillation

Performing this test at various speeds,  $V$ , and periods,  $\tau$ , will produce a variation in lateral speed,  $v$ ,  $Y_v$ ,  $Y_\delta$ ,  $N_v$ , and  $N_\delta$  are found by performing a Fourier analysis on the lateral force and yaw moment, and plotting the sway amplitudes against the sway velocity

amplitude. Note:  $Y_{\delta}$  is the inertial swaying load that is equal to the mass of the model plus its added mass in sway.

### Pure Yaw Tests

In this test, the model is rotated during manoeuvre so that its heading is always tangent to the sway path according to:

$$\begin{aligned} \dot{x} &= V \\ \dot{y} &= -Y_o \omega \sin(\omega t) \\ \phi &= \tan^{-1} \left[ \frac{-Y_o \omega}{V} \sin(\omega t) \right] \\ r &= \frac{d\phi}{dt} = -\frac{Y_o \omega^2 V}{V^2 + v^2} \cos(\omega t) \end{aligned}$$

Where:  $\dot{x} = V$  = surge velocity  
 $\dot{y} = v$  = sway velocity  
 $Y_o$  = sway amplitude  
 $\omega$  = circular frequency  
 $t$  = time  
 $\phi$  = yaw angle  
 $r$  = yaw rate

Because the heading is always tangent to the path, sway velocity,  $v$ , is equal to zero; therefore the model experiences only a variable rotational flow. The resulting forces and moments are the result of the rotational velocity and acceleration. Testing a number of velocities,  $V$ , and periods,  $\tau$ , yields a variation in yaw rate,  $r$ . The derivatives,  $Y_r$ ,  $Y_{\delta}$ ,  $N_r$ , and  $N_{\delta}$  are found by performing a Fourier analysis on the lateral force and yaw moment, and plotting the amplitudes against the yaw rate amplitude.

### Pure Yaw with Drift

These tests are performed to determine cross flow derivatives. They are performed over a range of drift angles and consist of a combination of the pure yaw and static drift tests described above. In this manoeuvre, the model experiences a pure yawing motion with a constant lateral cross-flow velocity. The yaw angle is given by:

$$\phi = \tan^{-1} \left[ \frac{Y_o \omega}{V} \sin(\omega t) \right] + \beta, \text{ where: } \beta = \text{drift angle}$$

Note: See Pages 26 and 27 for variable definition.

## Turning Circle Tests

The response of a ship to the deflection of its rudder(s) and the resulting forces and moments produced by the rudder(s) can be divided into an initial transient phase and a static phase. The transient phase occurs at the initiation of a turn and persists until the surge, sway, and yaw accelerations go to zero. At this time the manoeuvre enters the static phase, which is characterized by constant surge, sway, and yaw velocities. The steady turning radius is measured (or predicted) during the static turning phase.

## Turning Circle Predictions

Once the coefficients of the equations of motion for the model are known, its turning circle can be predicted for either open water or ice.

For open water turning circle tests,  $\dot{\delta}$  and  $\ddot{\delta}$  are equal to zero, therefore:

$$-Y'_v v' - (Y'_r - m')r' = Y'_\delta \delta$$

$$-N'_v v' - (N'_r - m'x'_G)r' = N'_\delta \delta$$

Since  $R = V/r$  and  $r' = \frac{rL}{V}$ , then  $r' = \frac{L}{R}$ . Then solving above equations simultaneously and substituting  $r' = \frac{L}{R}$  yields:

$$\frac{R}{L} = -\frac{1}{\delta} \left[ \frac{Y'_v(N'_r - m'x'_G) - N'_v(Y'_r - m')}{Y'_v N'_\delta - N'_v Y'_\delta} \right]$$

Note: See pages 26 and 27 for variable definitions.

For turning circles in ice,  $Y'_v$  is much greater than  $N'_v$  because the force acts approximately at amidships. Further, if  $x'_G$  is ignored then the above equation reduces to:

$$\frac{R}{L} = -\frac{1}{\delta} \left[ \frac{N'_r}{N'_\delta} \right]$$

or

$$R = -\frac{V}{\delta} \left[ \frac{N'_r}{N'_\delta} \right]$$

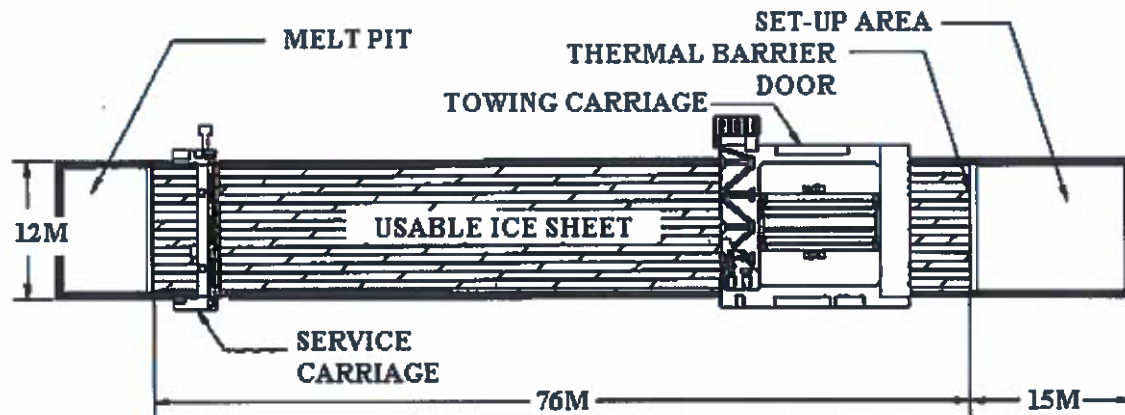
## 6. FACILITIES AT IOT

Detailed descriptions for ice tank, refrigerated system, towing carriage and service carriage are introduced by Joñes (1986).

### 6.1. Ice Tank

The useable area of the tank for ice testing is 76 m long, 12 m wide and 3 m deep. In addition, a 15 m long setup area located at one end of the tank is separated from the main ice testing area by a thermal door to allow equipment preparation while the ice sheet is prepared, as shown in Figure 8.

The tank is constructed and supported by four rows of concrete column. Epoxy painting on the tank wall provides corrosion protection from doped solution. The thermal door is composed of three insulated plates and it is counterbalanced with counter weights. A melting pit is located at the opposite side of the set-up area to melt the used ice sheet while growing a new ice sheet for next test. On the bottom of the tank, six lines of pipes are longitudinally laid releasing air bubbles to stir up the tank solution. Another air bubble system is used to correct density for CD-EG/AD/S ice during the ice growth.



### ICE TANK 3.0 METRES DEEP

Figure 8: Schematic diagram of the ice tank (after IOT standard test method, 2000)

## 6.2. Refrigeration System

The ammonia refrigeration system is designed to produce an ice sheet at a rate of 3.5 mm/hour with a freezing temperature of  $-25^{\circ}\text{C}$ . To-date, the maximum thickness of the ice sheets tested is about 160 mm. The refrigeration system is composed of compressors, evaporators and condensers. Five compressor units, including two boosters, two high stage and one single stage units, are used. The compressor units have a combined maximum capacity of 1200kW. Twenty-four evaporators installed on the ceiling are used to maintain air temperature to  $-20^{\circ}\text{C}$  during ice growth. Compressor output, evaporators and fan speed are computer controlled to maintain constant ice temperature for uniform ice growth.

A total of 12 thermocouples are used to measure the air temperature at 20 mm from the ice surface. During the warm-up period of ice tempering process, these thermocouples are raised to about 1.2 m above the ice sheet to avoid undue interference to the ice tempering. During the model tests these thermocouples are raised up to the roof to be out of the way of the carriage and the measurements of ice temperature are performed manually by using other probes in the ice tank. Typical range of the temperature for model tests in the ice tank is from zero to two degrees.

The rate of water chilling is about  $-0.18^{\circ}\text{C}/\text{hour}$ . Once the water temperature reached  $0^{\circ}\text{C}$ , the water chilling system is turned off. During the water chilling period, air temperature is kept to  $-5^{\circ}\text{C}$  or below. The air cooling rate is about  $-5^{\circ}\text{C}/\text{hour}$ , and once the temperature is at  $-20^{\circ}\text{C}$ , the seeding process is started. Perimeter heating inside the ice tank wall is turned on during the air cooling process (about 2-3 hours prior to seeding process) and then turned off at the end of air cooling process (about 30 min prior to seeding process).

The objective of the seeding process is to nucleate a thin layer of fine-grained ice skim on the water surface. Warm water, which is about  $30^{\circ}\text{C}$ , is sprayed by using compressed air from the service carriage that moves at a speed of 0.04m/s down the tank (from the thermal door to the melting pit). During this time, the ice booms of the service carriage are lowered about 10-15 centimeters into the water to remove any ice that formed during the initial cooling period while seeding for the ice sheet. The seeding process takes about 30 minutes and the evaporator fans are turned off during this period. After the seeding process, the freeze process is started.

A typical freezing process (ice growth process) is carried out at a temperature of  $-18$  to  $-22^{\circ}\text{C}$ . During this process, ice grows downward forming the typical columnar structure. The growth rate is about 2.5 mm/hour. It is noted that the ice grows not only in the freezing process but also in the tempering process. For example, a target ice thickness of 40 mm ice would require, 12 hours of freezing time to produce a 31 mm thick ice before the onset of the tempering process, and it continues to grow to target thickness during the tempering period. Therefore, if the growth of ice includes the growth during tempering process, the growth rate for the freeze cycle can be about 3.3 mm/hour.

The tempering process is used to reduce ice strength to the target value. At the end of freezing process, the refrigeration system is turned off and the air temperature rises naturally at a rate of about 5 °C/ hour. Once the air temperature is at -7 °C, the blast heaters are used to raise the temperature up to 2 °C rapidly. The tempering process is carried out at this air temperature. Figure 9 shows a typical temperature record measured during preparation of an ice sheet. It is cautioned that the temperature after tempering process is not valid as the thermocouples are raised up to the roof during this time.

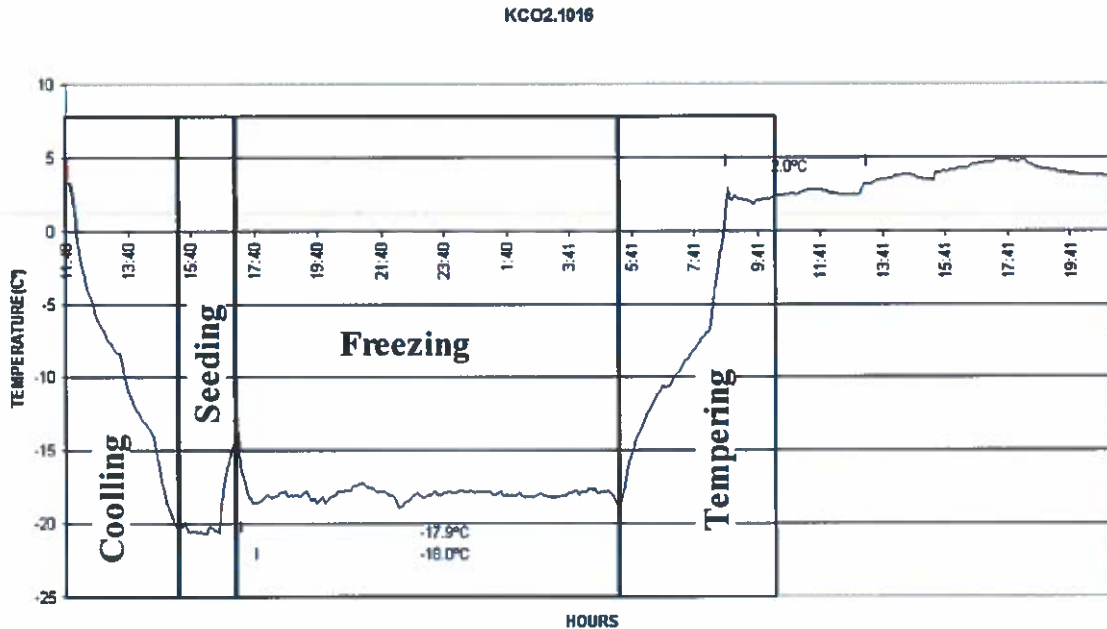


Figure 9: Temperature survey during the preparation of ice sheet

### 6.3. Towing Carriage (Main Carriage)

The towing carriage is an 80 tonnes steel structure made of low temperature steel (ABS EH36), and it is designed for an operating temperature as low as -40 °C as shown in Figure 10. The operating speed ranges from 0.0002 to 4.0 m/s with four sets of bogey wheel allowing a carriage speed up to 2.0 m/s and two sets of rack and pinion system allowing a carriage speed up to 4.0 m/s. The test frame on the carriage can move transversely using the transverse motor (3.7 kW) and vertically using the elevate motor (5.5 kW) to provide flexibility in positioning the model at various locations across the width of the tank and respective to the waterline. A 12 m ship model with a 12000 kg displacement has been tested in the tank. The carriage is designed to withstand ice loads up to 60 kN at the tank's center line, and up to 30 kN at the quarter points (3 m offset from the centerline). It is designed to withstand a load up to 2 kN at the vertical direction, and a 10 kN side thrust. The carriage speed is computer controlled and programmed to allow up to six individual speeds to be tested during one run. This includes the setting of carriage acceleration, deceleration and test distance for each test speed. The control room

houses the carriage drive control system, video system, data acquisition system, and the data storage system. Test data can be analyzed both on-line and offline.

An underwater carriage<sup>o</sup> can be attached or detached from the carriage by using<sup>f</sup> a vertical mast. The underwater carriage provides the various mounting sites for a number of underwater cameras. The operating speed is limited to 1.0 m/s in order to avoid the blockage effect at high speed.

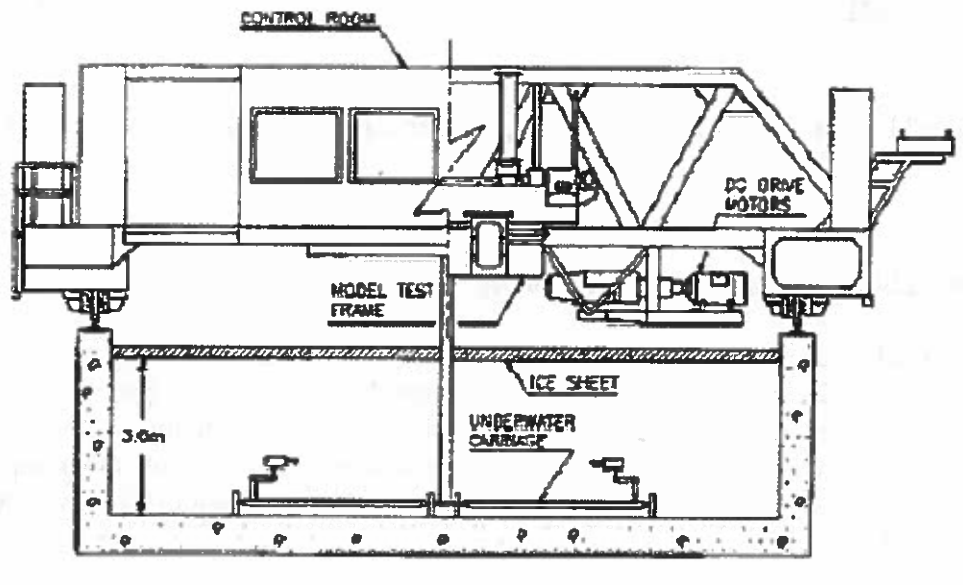


Figure 10: Front view of main carriage (15m long, 14.2 m wide, and 3.96 m high; after IOT standard test method, 2000)

#### 6.4. Service Carriage (Second Carriage)

The service carriage is an independent hydraulically operated unit and it is useful for ice control and sampling. The main duties of the service carriage are to allow in-situ measurement of the ice properties, ice sheet management, production of pack ice and ice ridges, clearing of broken ice into the melting pit after tests, and seeding of ice. The carriage has three sectioned working platforms and ice booms which can be independently controlled. The individual platform can adjust its height relative to the ice surface, and the booms can be tilted from 0 to 90 degrees for ice pushing or breaking. The service carriage is a 24 tonnes steel structure with four wheels and it has a speed up to 0.5 m/s. The front view is shown in Figure 11.

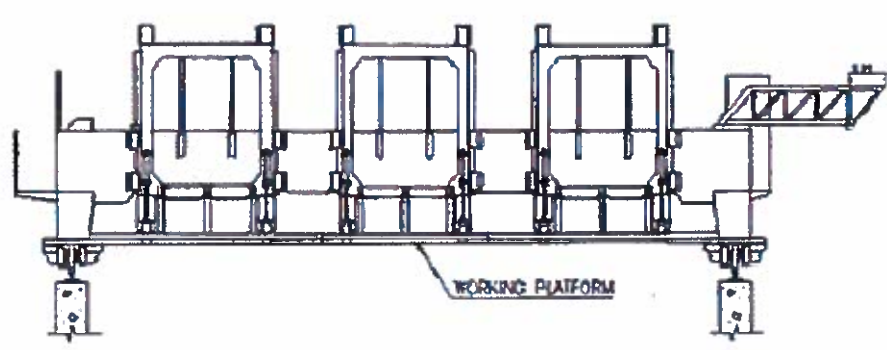


Figure 11: Front view of service carriage (after IOT standard test method, 2000)

### 6.5. Air Bubble System to Correct Density

In order to achieve the appropriate density for the model ice, air bubbling system has been installed on the bottom of the ice tank (Figure 12). This system provides very tiny air bubbles released from 0.037 mm holes 0.5 cm apart along the length of the pipe. The pipe is 1.4 cm in diameter and lies transversely and moves back and forth across the longitudinal direction of the tank. Typical operating speed is about 0.4 m/min and the system is used during the freezing process.

The air bubble system for density correction is described by Spencer and Timco (1990) and summarized in Section 3.5. The density of normal EG/AD/S model ice is about  $0.94 \text{ Mg/m}^3$ , and the CD-EG/AD/S model ice has a density of about  $0.87 \text{ Mg/m}^3$ .

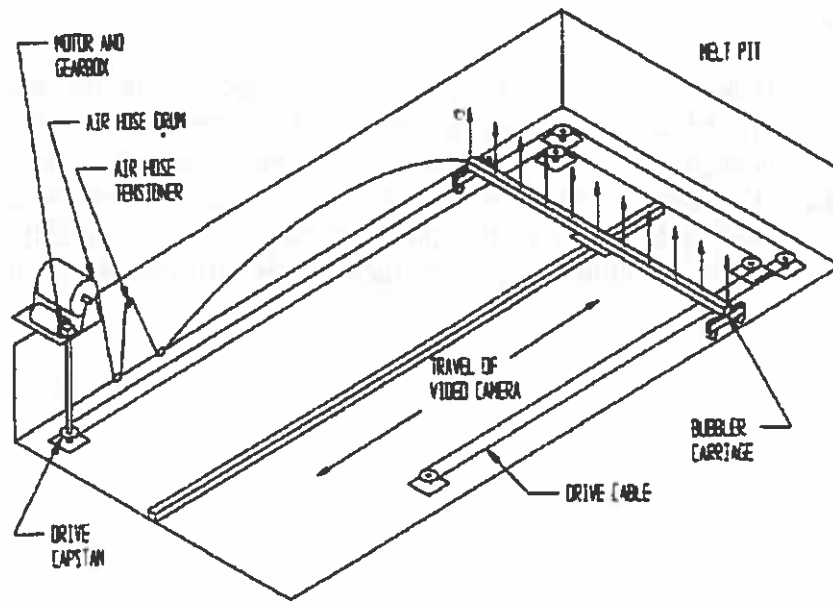


Figure 12: Air bubble system (after Spencer and Timco 1990)

## 7. SUMMARY

The aim of this study is to assist MOERI's new ice model basin to employ model ice and methodologies for model tests. This study reviews the state-of-the-art ice modeling techniques, mechanical properties of model ices and model test methodologies used in existing ice tanks. This report will help to understand the refrigerated model ice and model tests in an ice tank. As it is the planning stage of the MOERI's ice tank construction, detailed information of the IOT facilities is provided for their reference purpose.

## 8. REFERENCE

- Atkins, A., 1975, "Icebreaking Modeling," *Journal of Ship Research*, Vol. 19, No. 1, pp. 40-43.
- Atkins, A. and Caddell, R., 1974, "The Laws of Similitude and Crack Propagation," *Int. J. Mech. Sci.*, Vol. 16, pp. 541-548.
- Borland, S., 1988, "The Growth of EG/AD/S Model Ice in a Small Tank," *Proc. of the 7<sup>th</sup> International Conference on Offshore Mechanics and Arctic Engineering*, Houston, TX, Vol. 4, pp. 47-53.
- Cammaert, A. and Muggeridge, D., 1988, *Ice Interaction with Offshore Structures*, New York, Van Nostrand Reinhold.
- Colbourne, D. and Lever, J., 1992, "Development of a Component-Based Scaling System for Ship-Ice Model Tests," *Journal of Ship Research*, Vol. 36, No. 1, pp. 77-87.
- Cox, G. and Weeks, W., 1982, "Equations for Determining the Gas and Brine Volumes in Sea Ice Samples," CRREL Report 82-30, Hanover, N.H., USA.
- Dykins, T., 1971, "Ice Engineering- Material Properties of Saline Ice for a Limited Range of Conditions," Technical Report R720, Naval Civil Engineering Laboratory, California.
- Enkvist, E., 1983, "A Survey of Experimental Indications of the Relation between the Submersion and Breaking Components of Level Ice Resistance to Ships," *Proc. of the 7<sup>th</sup> POAC*, pp. 484-493
- Enkvist, E., 1972, "On the Ice Resistance Encountered by Ships Operating in the Continuous Mode of Icebreaking," *Swedish Academy of Engineering Sciences in Finland*, Report No. 24, Helsinki, Finland.
- Enkvist, E. and Makinen, S., 1984, "A Fine-Grain Model-Ice," *Proc. of the 7<sup>th</sup> IAHR Ice Symposium*, Hamburg, Germany, Vol. 2, pp. 217-227.
- Ettema, R., 1986, "Research Needs for Physical Modeling in Ice Engineering: Reflections from a University Ice tank," *Cold Regions Science and Technology*, Vol. 13, pp. 57-65.
- Evers, K. and Jochmann, P., 1993, "An Advanced Technique to Improve the Mechanical Properties of Model Ice Developed at the HSVA Ice Tank," *Proc. of the 12<sup>nd</sup> POAC*, Hamburg, Vol. 2, pp. 877-888.
- Gagnon, R., and Jones, S. J., 2001, "Elastic Properties of Ice," Chapter 9 of *Handbook of Elastic Properties of Solids, Liquids and Gases*, ed. Levy, Bass and Stern, Vol. III: Elastic

Properties of Solids: Biological and Organic Materials, Earth and Marine Sciences, Academic Press, pp. 229-257.

Gow, A., 1984, "Crystalline Structure of Urea Ice Sheets Used in Modeling Experiments in the CRREL Test Basin," U.S. Army CRREL Report 84-24, Hanover, N.H., USA.

Hirayama, K., 1983, "Properties of Urea-Doped Ice in the CRREL Test Basin," U.S. Army CRREL Report 83-8, Hanover, N.H., USA.

IOT, 2000, "Standard Test Method for Resistance in Ice," IOT Standard, 42-8595-S/TM7

ITTC, 2005, "The Specialist Committee on Ice: Final Report and Recommendations to the 24<sup>th</sup> ITTC," 24<sup>th</sup> International Towing Tank Conference, Edinburgh, UK.

ITTC, 1999, "The Specialist Committee on Ice: Final Report and Recommendations to the 22<sup>nd</sup> ITTC," 22<sup>nd</sup> International Towing Tank Conference, Seoul and Shanghai, Korea and China.

ITTC, 1996, "Performance in Ice-Covered Waters Committee: Final Report and Recommendations to the 21<sup>st</sup> ITTC," 21<sup>st</sup> International Towing Tank Conference, Trondheim, Norway.

Jalonen, R. and Ilves, L., 1990, "Experience with a Chemically-Doped Fine Grained Model Ice," Proc. of the 10<sup>th</sup> IAHR Ice Symposium, Espoo, Finland, Vol. 2, pp. 639-651.

Jones, S. J., 2006, "Comparison of the Strength of Iceberg and Other Freshwater Ice and the Effect of Temperature," Report Number TR-2006-07, Institute for Ocean Technology, National Research Council Canada.

Jones, S. J., 1986, "Canada's New Ice Tank," Proc. of the 21<sup>st</sup> ATTC, Washington D.C., pp. 315-319.

Jones, S. J., Kriby, C., Meadus, C., Tucker, W., Gagnon, J., and Elder, B., 2001, "Sea Ice Properties on the USCGC HEALY Ice Trials," Proc. of the 16<sup>th</sup> POAC, Ontario, Canada, pp. 845-954.

Jones, S., Spencer, D., and McKenna, R., 1994, "Icebreaking Performance from Model Scale Tests," ICETECH'94, Calgary, pp. H1-H19.

Jones, S. J. and Lau, M., 2006, "Propulsion and Maneuvering Model Tests of the USCGC Healy in Ice and Correlation with Full-Scale," International Conference on Performance of Ships and Structures in Ice, 16-19 July, Banff, Alberta.

Kashteljan, V., Poznjak, I., and Ryvlin, A., 1968, "Ice Resistance to Motion of a Ship," Sudostroenie, Leningrad.

- Kovacs, A., 1996a, "Sea Ice: Part I. Bulk Salinity Versus Ice Floe Thickness," CRREL Report 96-7, Hanover, N.H., USA.
- Kovacs, A., 1996b, "Sea Ice: Part II. Estimating the Full-Scale Tensile, Flexural, and Compressive Strength of First-Year Ice," CRREL Report 96-11, Hanover, N.H., USA.
- Lainey, L. and Tinawi, R., 1984, "The Mechanical Properties of Sea Ice-A Compilation of Available Data," Canadian Journal of Civil Engineering, Vol. 11, pp. 884-923.
- Lau, M. and Derradji-Aouat, A., 2004, "Preliminary Modeling of Ship Maneuvering in Ice," 25<sup>th</sup> Symposium on Naval Hydrodynamics, St. John's, Newfoundland.
- Lewis, J. and Edwards, R., 1970, "Predicting Icebreaking Capabilities of Icebreakers," Naval Engineering Division, Report No. 2, U.S. Coast Guard Headquarters.
- Marineering Limited, 1997, "The Development and Commissioning of a Large Amplitude Planar Motion Mechanism for Maneuvering of Ships in Ice and Open Water: Volume 1-Main Report," NRC/IMD Report CR-1997-05 Vol. 1 of 3, Institute for Ocean Technology, National Research Council of Canada, St. John's, NL.
- Mellor, M., 1986, "Mechanical Behavior of Sea Ice," The Geophysics of Sea Ice, Edited by Norbert Untersteiner, NATO ASI Series, Series B: Physics Vol. 146, pp.165-282.
- Michel, B., 1978, *Ice Mechanics*, Les Presses de l'Universite de Laval, Quebec.
- Moslet, P., 2007, "Field Testing of Uniaxial Compression Strength of Columnar Sea Ice," Cold Regions Science and Technology, Vol. 48, Issue 1, pp. 1 – 14.
- Molyneux, W., 1989, "Self-Propulsion Experiments for Icebreakers in Ice and Open Water," 22nd American Towing Tank Conference, St. John's, Nfld., pp. 326-331.
- Molyneux, W., Williams, F. M., and Hoffmann, K., 1998, "Evaluation of Performance Limitations for Ships Navigating to and from Voisey's Bay Part 5; Maneuvering Experiments in Level, Pack and Rubble Ice," Institute for Ocean Technology, Report TR-1998-07, St. John's, NL.
- Moore, C., Veitch, B., Bose, N., Jones, S. J., and Bugden, A., 2001, "Effects of Strain Rate and Temperature on the Uniaxial Compressive Strength of EG/AD/S CD Model Ice," Proc. of the 16<sup>th</sup> POAC, Ontario, Canada, pp. 1423-1432.
- Narita, S., Inoue, M., Kishi, S., and Yamauchi, Y., 1988, "The Model Ice of the NKK Ice Model Basin," Proc. of the 9<sup>th</sup> IAHR Ice Symposium, Sapporo, Japan, Vol. 1, pp. 782-792.
- Nortala-Hoikkanen, A., 1990, "FGX Model Ice at the MASA-Yards Arctic Research Centre," Proc. of the 10<sup>th</sup> IAHR Ice Symposium, Espoo, Finland, Vol. 3, pp. 247-259.

- Parsons, B. and Snellen J., 1985, "Fracture Toughness of Fresh Water Prototype Ice and Carbamide Model Ice," Proc. of the 8<sup>th</sup> POAC, Vol. 1, pp. 128-137.
- Parsons, B., Snellen, J., Hill, B., 1986, "Physical Modeling and the Fracture Toughness of Sea Ice," 5th International Offshore Mechanics and Arctic Engineering Symposium, April 13-18, Tokyo, Japan, pp. 358-364.
- Poznjak, I. And Ionov, B., 1981, "The Division of Icebreaker Resistance into Components," Proc. of the 2<sup>nd</sup> ICETECH, Ottawa.
- Pratte, B and Timco, G., 1981, "A New Model Basin for the Testing of Ice-Structure Interactions," Proc. of the 6<sup>th</sup> POAC, pp. 857-866.
- Riska, K., Jalonen, R., Veitch, B., Nortala-Hoikkanen, A., and Wilkman, G., 1994, "Assessment of Ice Model Testing Techniques," Proc. of the 5<sup>th</sup> ICETECH, Calgary, pp. F1-F22.
- Schwarz, J., 1977, "New Developments in Modeling Ice Problems," Proc. of the 4<sup>th</sup> POAC, Vol.1, St. John's, NL, pp. 45-61.
- Shavaishtein, Z., 1971, "Experimental Studies in an Ice-Research Laboratory," Studies in Ice Physics and Ice Engineering, Proceeding Vol. 300, pp. 16-25.
- Shavaishtein, Z., 1959, "Laboratory for Studying Ice and Testing Models of Icebreakers and Ice Strengthened Vessels," Problemi Arktiki, Vol. 2, pp. 171-178 (in Russian).
- Schwarz, J., 1975, "On the Flexural Strength and Elastic of Saline Ice," Proc. of the 3<sup>rd</sup> IAHR Symp. on Ice Problems, Hanover, N.H., USA, pp. 373-386.
- Shi, Y., 2002, "Model Test Data Analysis of Ship Maneuverability in Ice," Master thesis, Memorial University of Newfoundland.
- Sodhi, D., Kato, K., Haynes, F., and Hirayama, K., 1982, "Determining the Characteristic Length of Model Ice Sheets," Cold Regions Science and Technology, Vol. 6, pp. 99-104.
- Spencer, D. and Hill, B., 1994, "Hi-E Model Ice: Improving the Elastic Modulus of Columnar Model Ice," Proc. of the 12<sup>th</sup> IAHR Ice Symposium, Trondheim, Norway, Vol. 1, pp. 426-435.
- Spencer, D. and Jones, S. J., 2001, "Model-Scale/Full-Scale Correlation in Open Water and Ice for Canadian Coast Guard "R-Class" Icebreakers," Journal of ship research, Vol. 45, No. 4, pp. 249-261.
- Spencer, D. and Timco, G., 1990, "CD Model Ice: A Process to Produce Correct Density Model Ice," Proc. of the 10<sup>th</sup> IAHR Ice Symposium, Espoo, Finland, Vol. 2, pp. 745-755.

- Spencer, D. and Williams, F. M., 1998, "Development of a New large Amplitude Planar Motion Mechanism at IMD," Proc. of the 25<sup>th</sup> ATTC, September, Iowa Institute for Hydraulic Research, Iowa City, pp. 6-13 ~ 6-18
- Timco, G., 1979, "The Mechanical and Morphological Properties of Doped Ice," Proc. of the 5<sup>th</sup> POAC, Trondheim, Norway, Vol. 1, pp. 719-739.
- Timco, G., 1980, "The Mechanical Properties of Saline-Doped and Carbamide (Urea)-Doped Model Ice," Cold Regions Science and Technology, Vol. 3, pp. 45-56.
- Timco, G., 1992, "Second Report of the IAHR Working Group on Ice-Modelling Materials," Proc. of the 11<sup>th</sup> IAHR Symp. on Ice Problems, Banff, Canada, pp.1527-1536.
- Timco, G., 1986, "EG/AD/S: A New Type of Model Ice for Refrigerated Towing Tanks," Cold Regions Science and Technology, Vol. 12, pp. 175-195.
- Timco, G., 1985, "Flexural Strength and Fracture Toughness of Urea Model Ice," Journal of Energy Resources Technology, Vol. 107, pp. 498-505.
- Timco, G., 1984, "Ice Forces on Structures: Physical Modeling Techniques," Proc. of the 7<sup>th</sup> IAHR Symp. on Ice Problems, Hamburg, Germany, Vol. 4, pp.117-150.
- Timco, G., 1983, "Uniaxial and Plane-Strain Compressive Strength of Model Ice," Annals of Glaciology, Vol. 4, pp. 289-293.
- Timco, G. and Frederking, R., 1982, "Flexural Strength and Fracture Toughness of Sea Ice," Cold Regions Science and Technology, Vol. 8, pp. 35-41.
- Timco, G. and Frederking, R., 1990, "Compressive Strength of Sea Ice Sheets," Cold Regions Science and Technology, Vol. 17, pp. 227-240.
- Timco, G. and Frederking, R., 1996, "A Review of Sea Ice Density," Cold Regions Science and Technology, Vol. 24, pp. 1-6.
- Timco, G. and O'Brien, S., 1994, "Flexural Strength Equation for Sea Ice," Cold Regions Science and Technology, Vol. 22, pp. 285-298
- Urabe, N, Iwasaki, T., and Yoshitake, A., 1980, "Fracture Toughness of Sea Ice," Cold Regions Science and Technology, Vol. 3, pp. 29-37
- Urabe, N. and Yoshitake, A., 1984, "Similitude Law of Ice Based on Fracture Mechanics," Proc. of the 3<sup>rd</sup> International Conference on Offshore Mechanics and Arctic Engineering, New Orleans, Louisiana, Vol. 3, pp. 178-182.

USACE, 2002, *Ice Engineering*, USACE Report EM 1110-2-1612, Department U.S. Army Corps of Engineers, Washington, DC.

Vaudrey, K., 1977, "Ice Engineering - Study of Related Properties of Floating Sea Ice Sheets and Summary of Elastic and Viscoelastic Analysis," Technical Report R860, Civil Engineering Laboratory, California.

Vaudrey, K., 1975, "Ice Engineering: Elastic Property Studies on Compressive and Flexural Sea Ice Specimens," Technical Note N-1417, Civil Engineering Laboratory, California.

Wang, Y., 1979a, "Crystallographic Studies and Strength Tests on Field Ice in the Alaskan Beaufort Sea," Proc. of the 5<sup>th</sup> POAC, Trondheim, Norway, Vol. 1, pp.651-665.

Wang, Y., 1979b, "Sea Ice Properties," In Technical Seminar on Alaskan Beaufort Gravel Island Design, Exxon, USA.

Weeks, W., 1982, "Physical Properties of the Ice Cover of the Greenland Sea," CRREL Special Report 82-28, Hanover, N.H., USA.

Weeks, W. and Anderson, D., 1958, "An Experimental Study of the Strength of Young Sea Ice," Trans. American Geophys. Union, Vol. 39, No. 4, pp.641-647.

Weeks, W. and Assur, A., 1967, "The Mechanical Property of Sea Ice," USA CRREL Monograph II-C3, Hanover, N.H., USA.

White, R. and Vance, G., 1967, "Icebreaker Model Tests," Naval Engineers Journal, Vol. 79, No. 4, pp. 601- 605.

Wilkman, G., Mattsson, T., and Niini, M., 2006, "First Experience in the Next Generation Ice Laboratory for Testing Ships and Structures," Proc. of the 25<sup>th</sup> International Conference on Offshore Mechanics and Arctic Engineering, June 4-9, Hamburg, Germany (CD-ROM).

Wilkman, G., Mattsson, T., Ponomarev, A., and Beliashov V., 1997, "Experience of a New Model Ice (MARC FG) Material at the Krylov Shipbuilding Research Institute (KSRI) Ice Basin," Proc. of the 16<sup>th</sup> International Conference on Offshore Mechanics and Arctic Engineering, Vol. 4, pp. 289-295.

Williams, F. M. and Waclawek, P., 1998, "Physical Model Tests for Ship Maneuvering in Ice," Proc. of the 25<sup>th</sup> ATTC, September, Iowa Institute for Hydraulic Research, Iowa City, pp. 9-11 ~ 9-16

Zufelt, J. and Ettema, R., 1996, "Model Ice Properties," CREEL Report 96-1, Hanover, N.H., USA.